Short-range correlation physics at low renormalization group (RG) resolution

Anthony Tropiano[1], Scott Bogner[2], Dick Furnstahl[1]

[1]Ohio State University, [2]Michigan State University

TU Darmstadt seminar

November 24, 2021

ajt, S.K. Bogner, and R.J. Furnstahl, arXiv:2105.13936

Phys. Rev. C ***104****, 034311 (2021)*

NUCLEI
Nuclear Computational Low-Energy Initiative

THE OHIO STATE UNIVERSITY

NSF

U.S. DEPARTMENT OF ENERGY

Short-range correlations

- Recent experiments have been able to isolate processes where short-range correlation (SRC) physics is dominant and well accounted for by SRC phenomenology
- How are short-range correlations defined?
  - Depends on the resolution scale!
  - Renormalization group (RG) resolution scale is set by Λ in the Hamiltonian $H(\Lambda)$
  - $\Lambda \sim$ max momenta in low-energy wave functions

High and low RG resolution

- SRC physics at high RG resolution
  - SRC pairs are components in the nuclear wave function with relative momenta above the Fermi momentum

High RG resolution

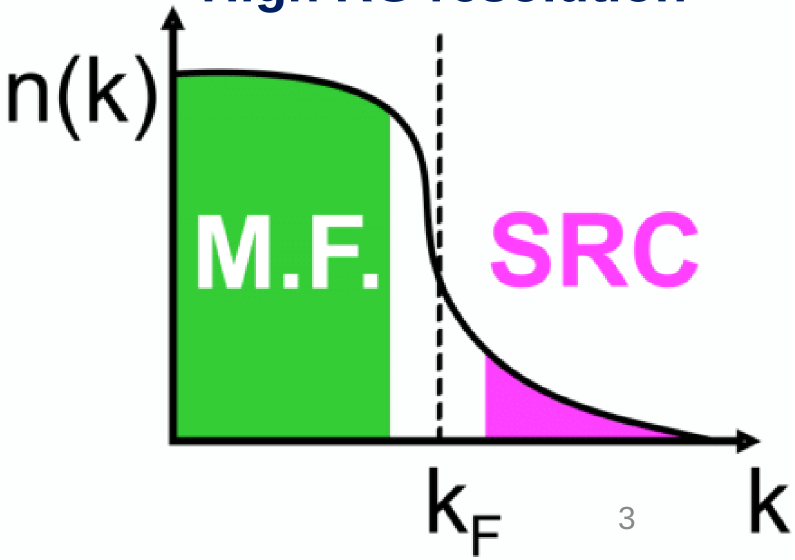

High and low RG resolution

- SRC physics at high RG resolution
  - SRC pairs are components in the nuclear wave function with relative momenta above the Fermi momentum
- SRC physics at low RG resolution
  - The SRC *physics* is shifted into the reaction operators from the nuclear wave function (which becomes soft)

Low RG resolution

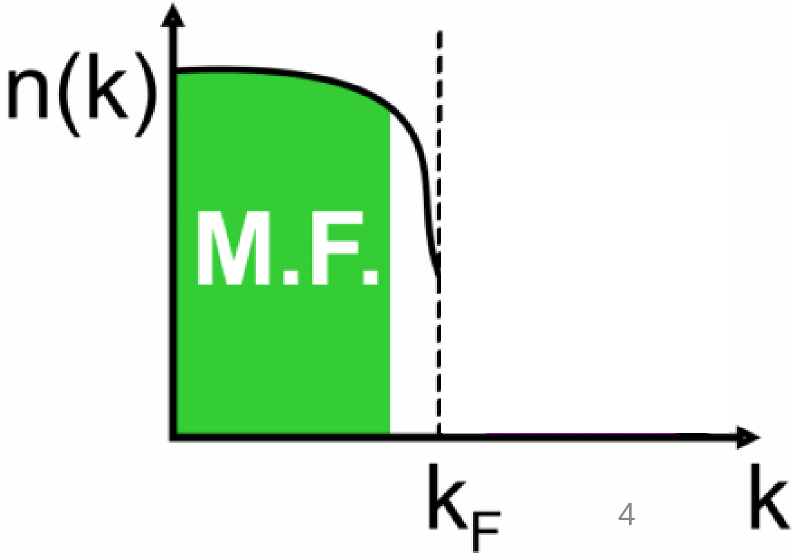

High and low RG resolution

- High RG resolution: One-body current operators with correlated wave functions

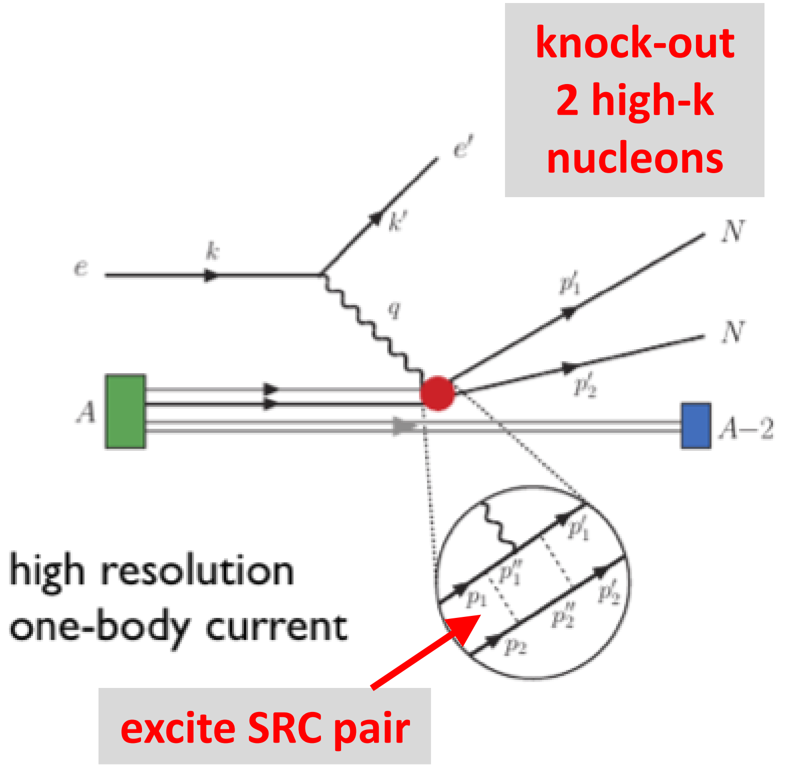

High and low RG resolution

- High RG resolution: One-body current operators with correlated wave functions
- Low RG resolution: Two-body current operators with uncorrelated wave functions
  - Operators do NOT become hard, which simplifies calculations!

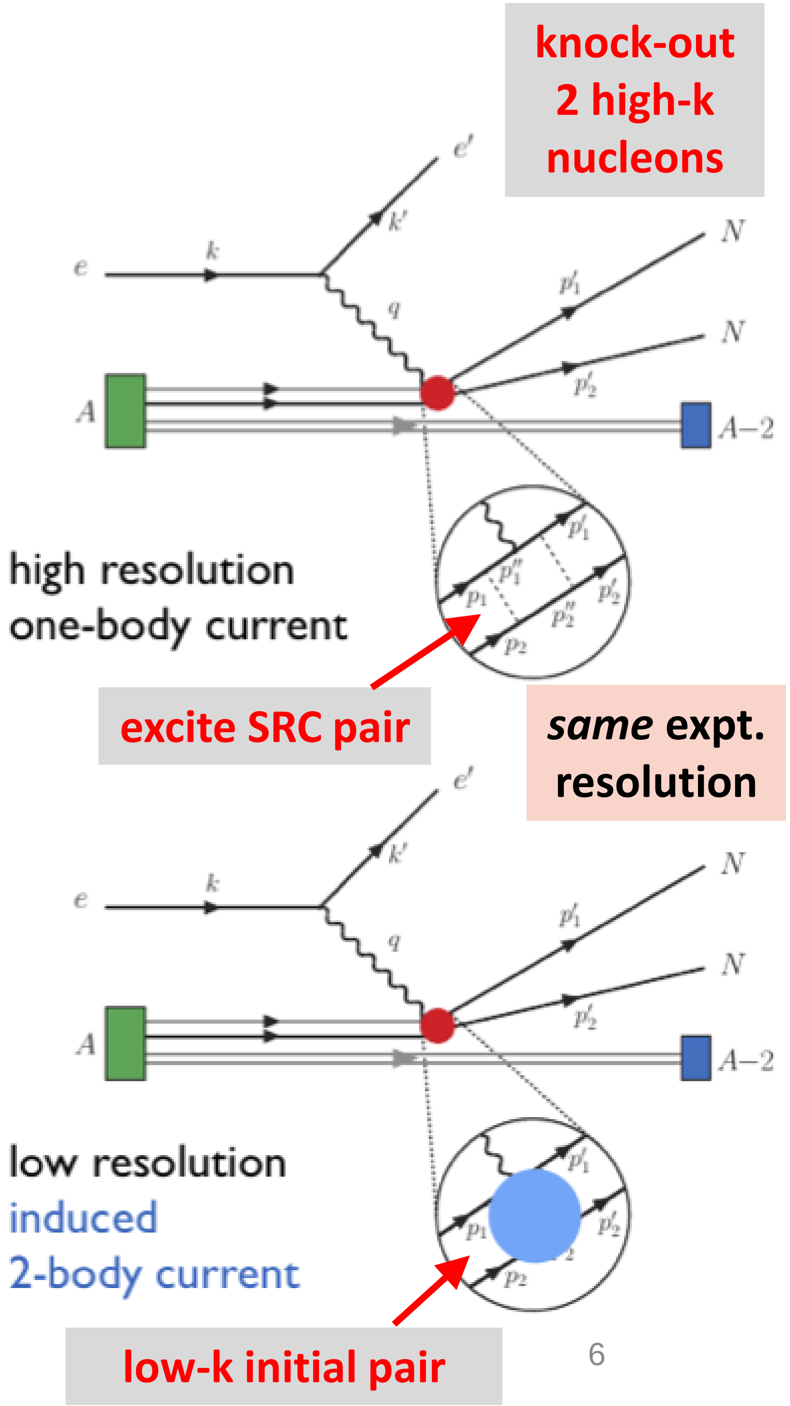

High and low RG resolution

- High RG resolution: One-body current operators with correlated wave functions
- Low RG resolution: Two-body current operators with uncorrelated wave functions
  - Operators do NOT become hard, which simplifies calculations!
- Experimental resolution (set by momentum of probe) is the same in both pictures
- Same observables but different physical interpretation!

knock-out
2 high-k
nucleons

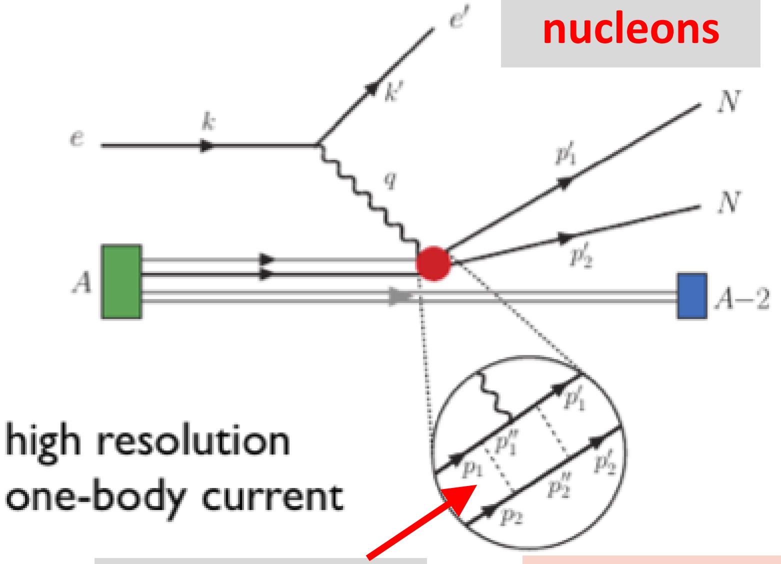

excite SRC pair

same expt.
resolution

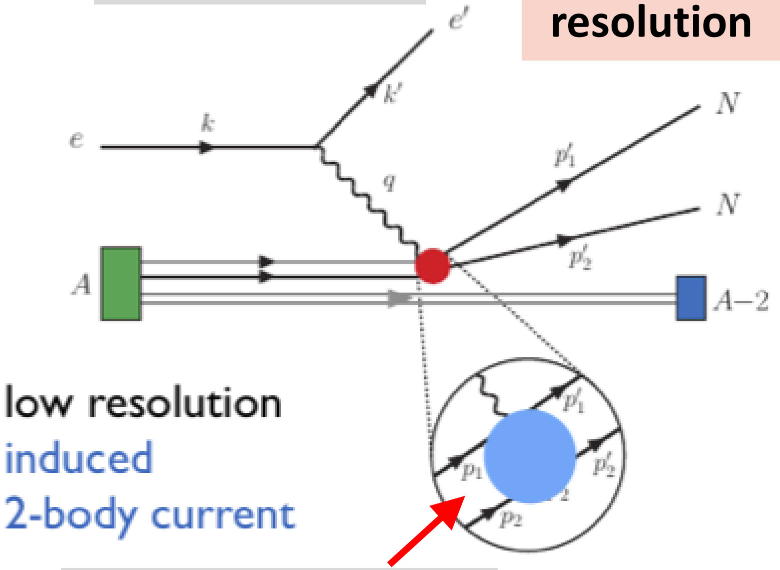

low-k initial pair

High and low RG resolution

- High RG resolution: One-body current operators with correlated wave functions
- Low RG resolution: Two-body current operators with uncorrelated wave functions
  - Operators do NOT become hard, which simplifies calculations!
- Experimental resolution (set by momentum of probe) is the same in both pictures
- Same observables but different physical interpretation!
- This talk:
  - How can SRC calculations be carried out at low RG resolution?
  - What can we describe with simple approximations?
  - Connections to existing SRC phenomenology (e.g., GCF/LCA)

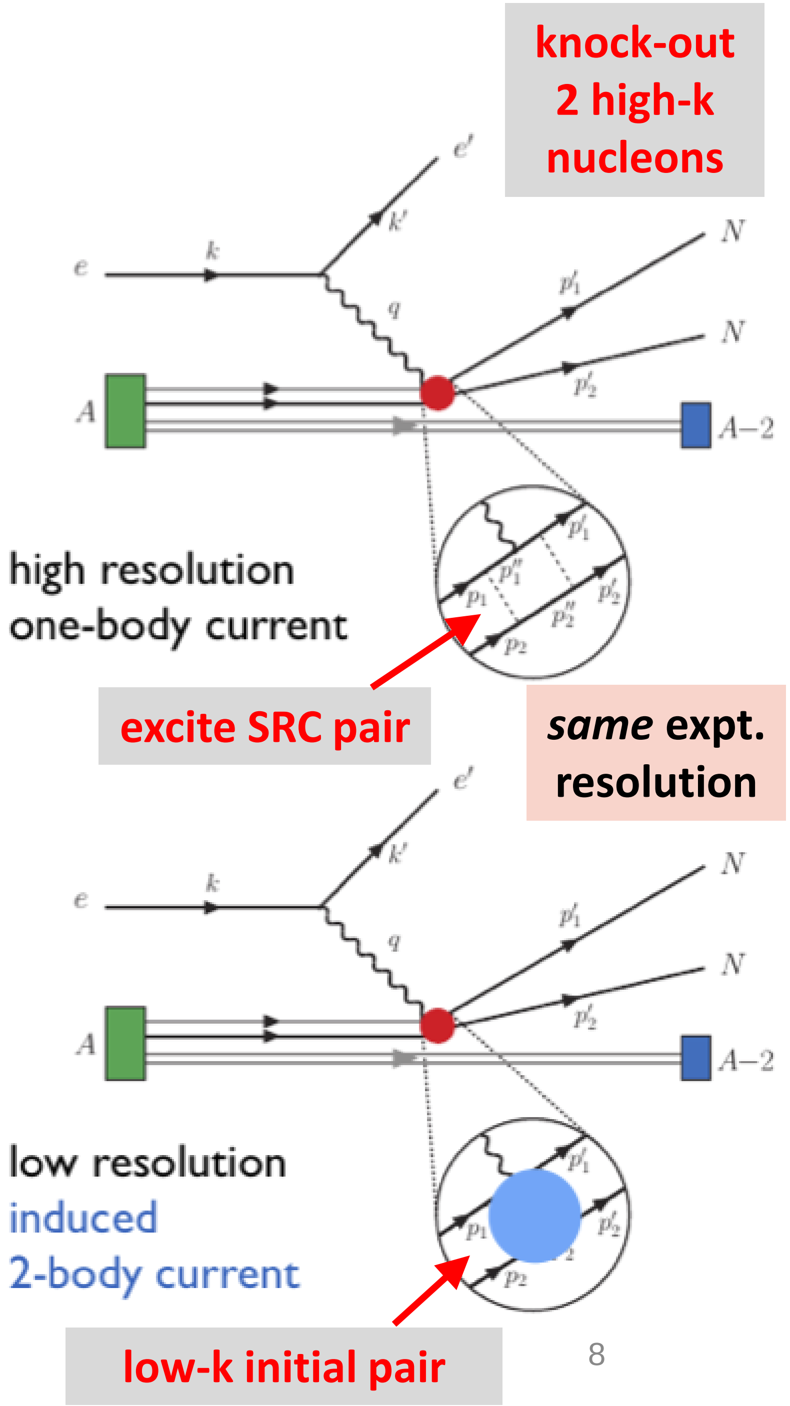

Similarity renormalization group

- Evolve to low RG resolution using the SRG
$$O(s) = U(s)O(0)U^{\dagger}(s)$$
where $s = 0 \rightarrow \infty$ and $U(s)$ is unitary
- SRG transformations decouple high- and low-momenta in the Hamiltonian

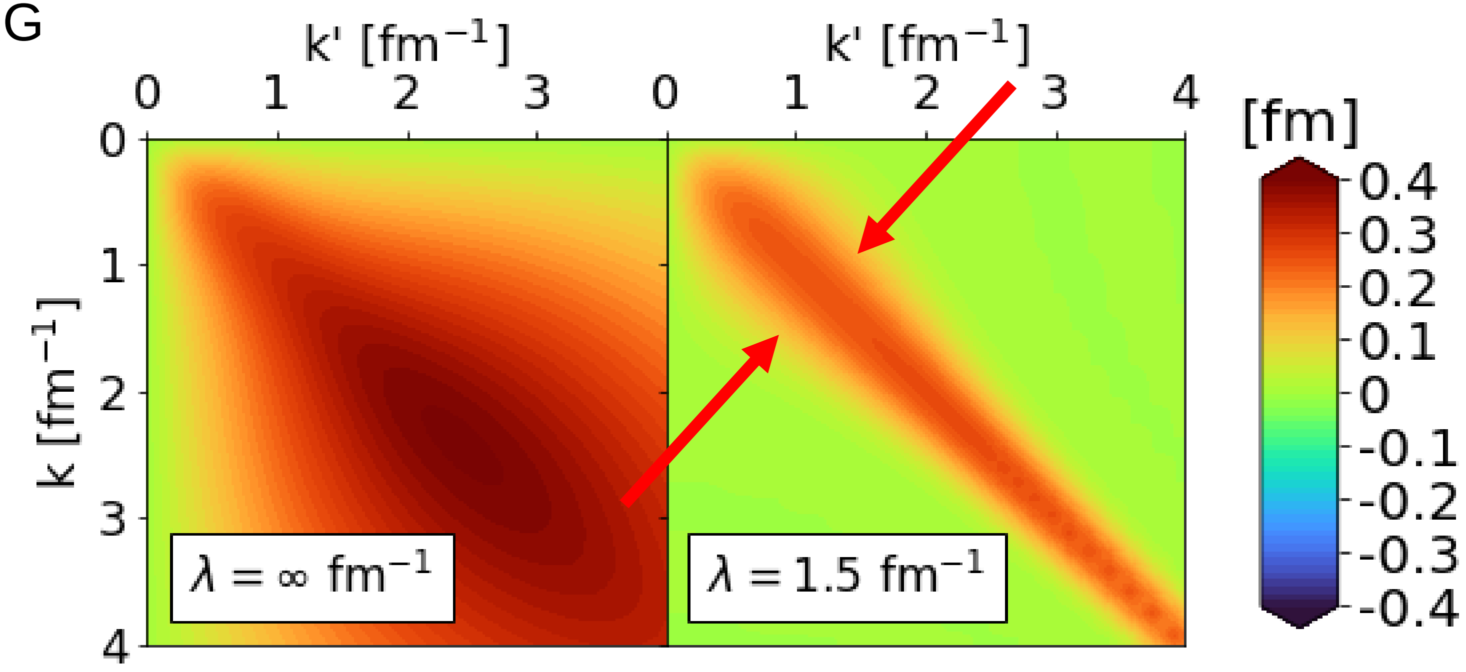

Fig. 1: Momentum space matrix elements of Argonne v18 (AV18) under SRG evolution in $^1P_1$ channel.

Similarity renormalization group

- Evolve to low RG resolution using the SRG
$$O(s) = U(s)O(0)U^\dagger(s)$$
where $s = 0 \to \infty$ and $U(s)$ is unitary
- SRG transformations decouple high- and low-momenta in the Hamiltonian
- In practice, solve differential flow equation
$$\frac{dO(s)}{ds} = [\eta(s), O(s)]$$
where $\eta(s) \equiv \frac{dU(s)}{ds} U^\dagger(s) = [G, H(s)]$ is the SRG generator
- Decoupling scale given by $\lambda = s^{-1/4}$

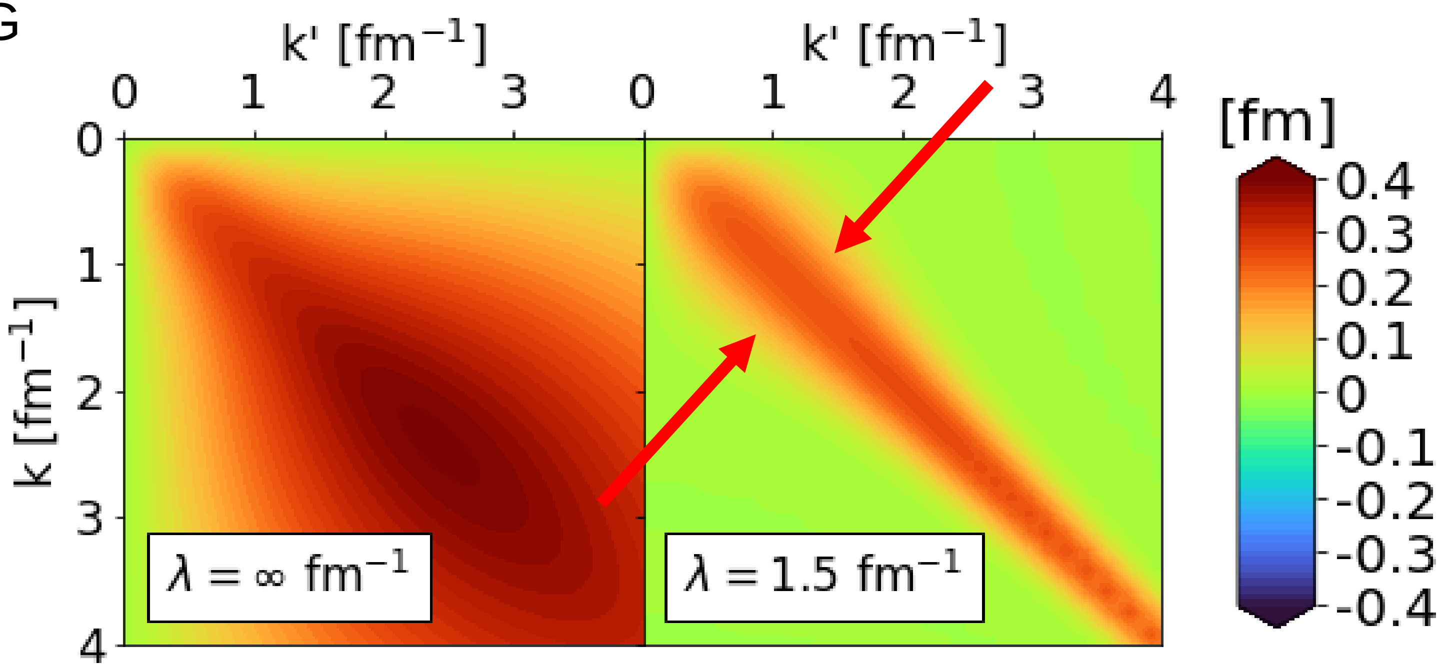

Fig. 1: Momentum space matrix elements of Argonne v18 (AV18) under SRG evolution in $^1P_1$ channel.

Similarity renormalization group

- AV18 wave function has significant SRC
- What happens to the wave function under SRG transformation?

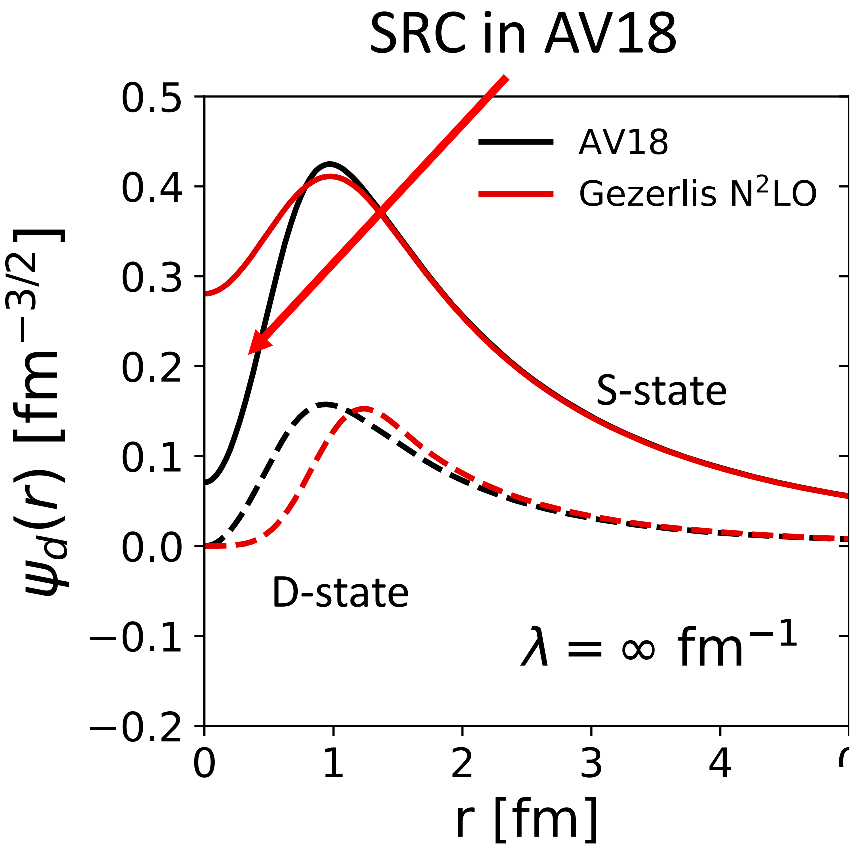

Fig. 2: SRG evolution of deuteron wave function in coordinate space for AV18 and Gezerlis N^{2}LO[1].

[1]A. Gezerlis et al., Phys. Rev. C **90**, 054323 (2014)

Similarity renormalization group

- SRC physics in AV18 is gone from wave function at low RG resolution
- Deuteron wave functions become soft and D-state probability goes down
- Observables such as asymptotic D-S ratio are the same

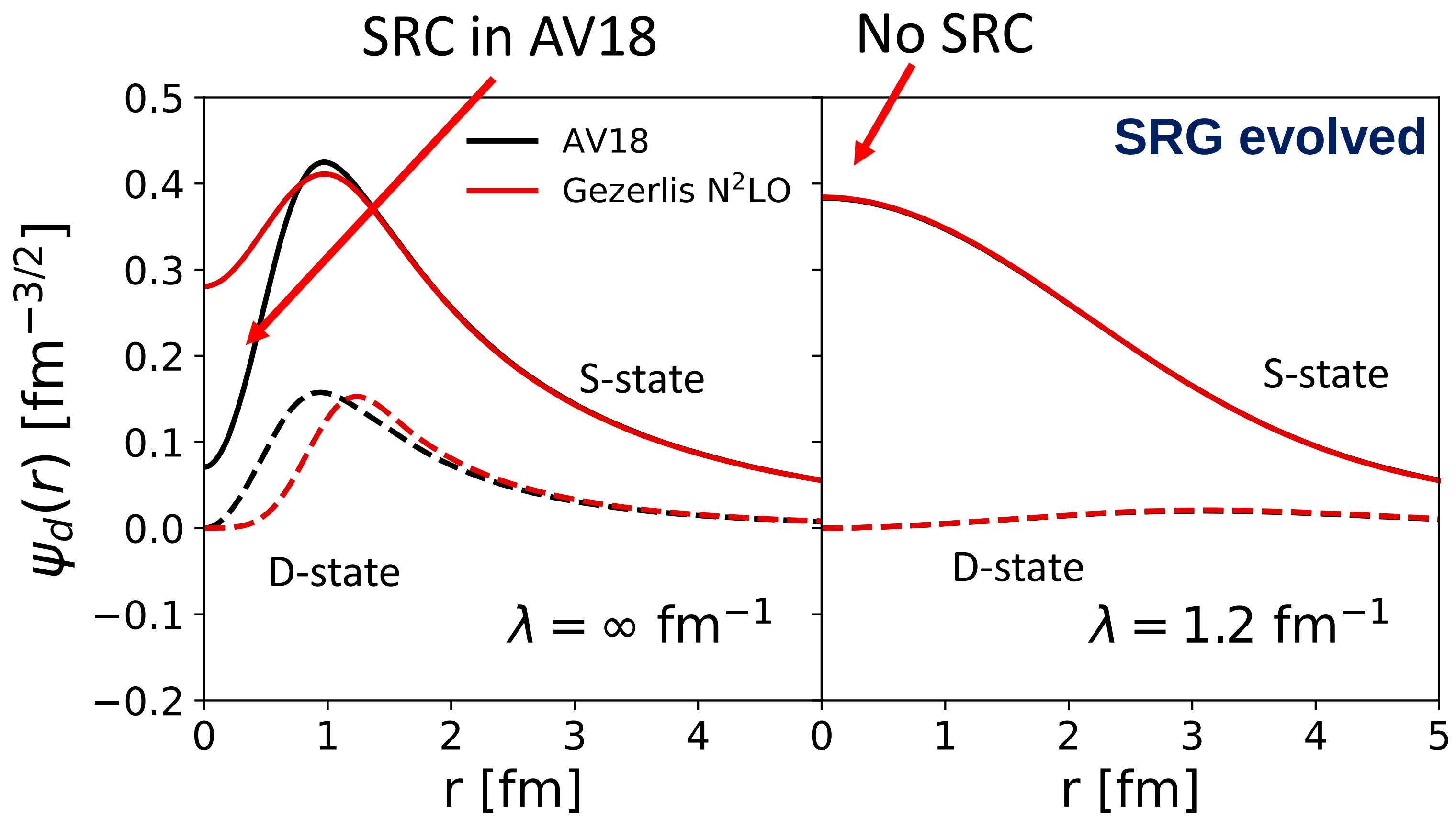

Fig. 2: SRG evolution of deuteron wave function in coordinate space for AV18 and Gezerlis N^{2}LO[1].

[1]A. Gezerlis et al., Phys. Rev. C **90**, 054323 (2014)

Operator evolution

- Soft wave functions at low RG resolution
- SRC physics shifts to the operators

$$\langle \psi_f^{hi} | U_\lambda^\dagger U_\lambda O^{hi} U_\lambda^\dagger U_\lambda | \psi_i^{hi} \rangle = \langle \psi_f^{low} | O^{low} | \psi_i^{low} \rangle$$

Operator evolution

- Soft wave functions at low RG resolution
- SRC physics shifts to the operators

$$\langle \psi_f^{hi} | U_\lambda^\dagger U_\lambda O^{hi} U_\lambda^\dagger U_\lambda | \psi_i^{hi} \rangle = \langle \psi_f^{low} | O^{low} | \psi_i^{low} \rangle$$

- **Example:** Calculate deuteron momentum distribution by evolving momentum projection operator $a_q^\dagger a_q$

$$n_d(q) = \langle \psi_d | a_q^\dagger a_q | \psi_d \rangle = \langle \psi_d^\lambda | U_\lambda a_q^\dagger a_q U_\lambda^\dagger | \psi_d^\lambda \rangle$$

Operator evolution

Fig. 3: Evolved momentum projection operator $U_\lambda a_q^\dagger a_q U_\lambda^\dagger$ for several λ values where $q = 3$ fm^{-1}.

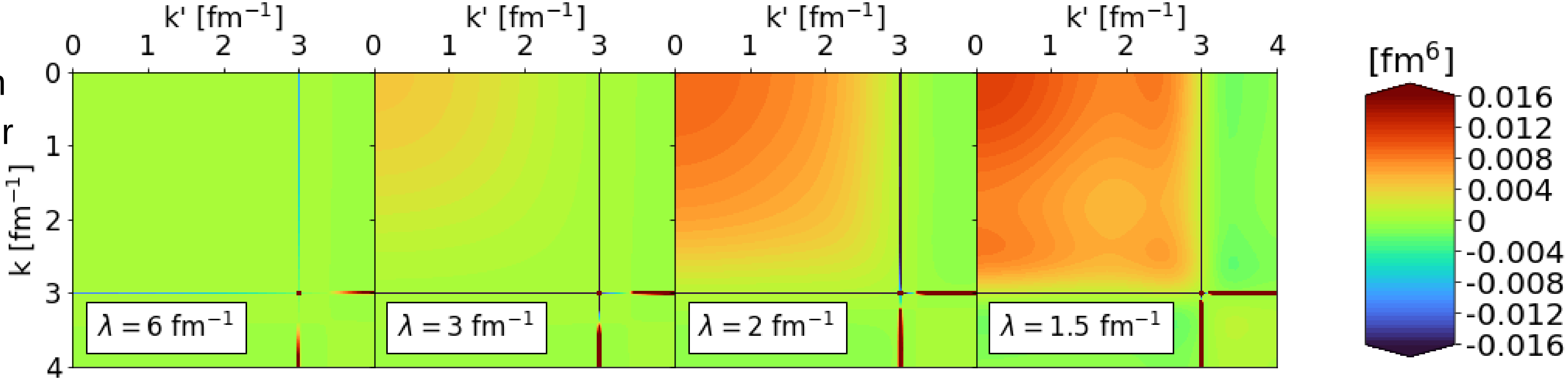

Operator evolution

Fig. 3: Evolved momentum projection operator $U_\lambda a_q^\dagger a_q U_\lambda^\dagger$ for several λ values where $q = 3$ fm⁻¹.

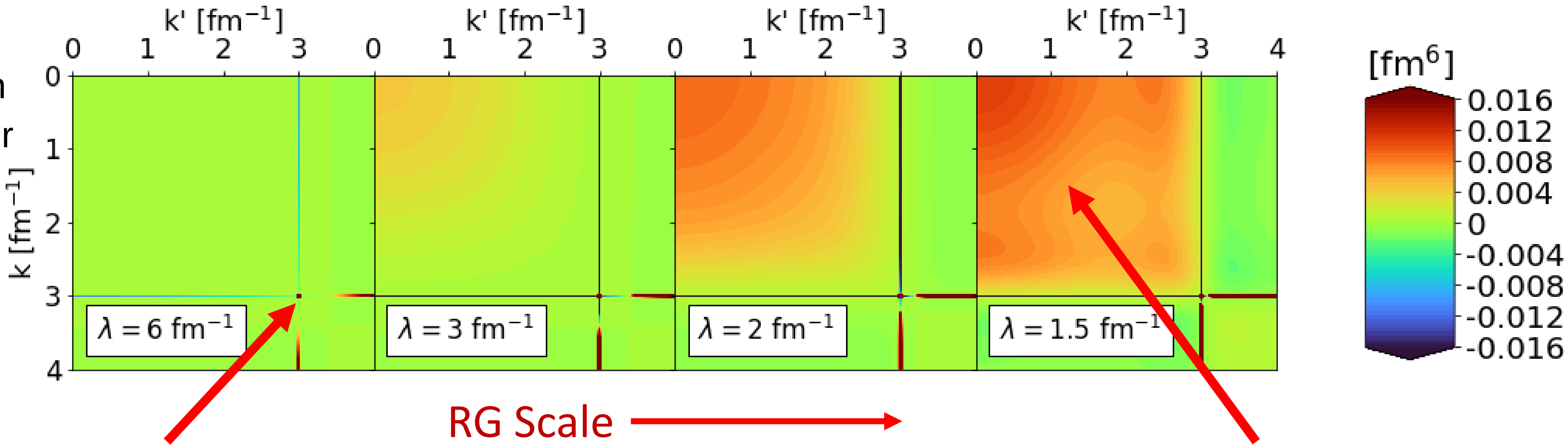

Bare operator is a discretized delta function in momentum space

$$\sim \delta(k-q)\delta(k'-q)$$

SRG evolution induces smooth, low-momentum contributions

Operator evolution

Fig. 3: Evolved momentum projection operator $U_\lambda a_q^\dagger a_q U_\lambda^\dagger$ for several λ values where $q = 3$ fm^{-1}.

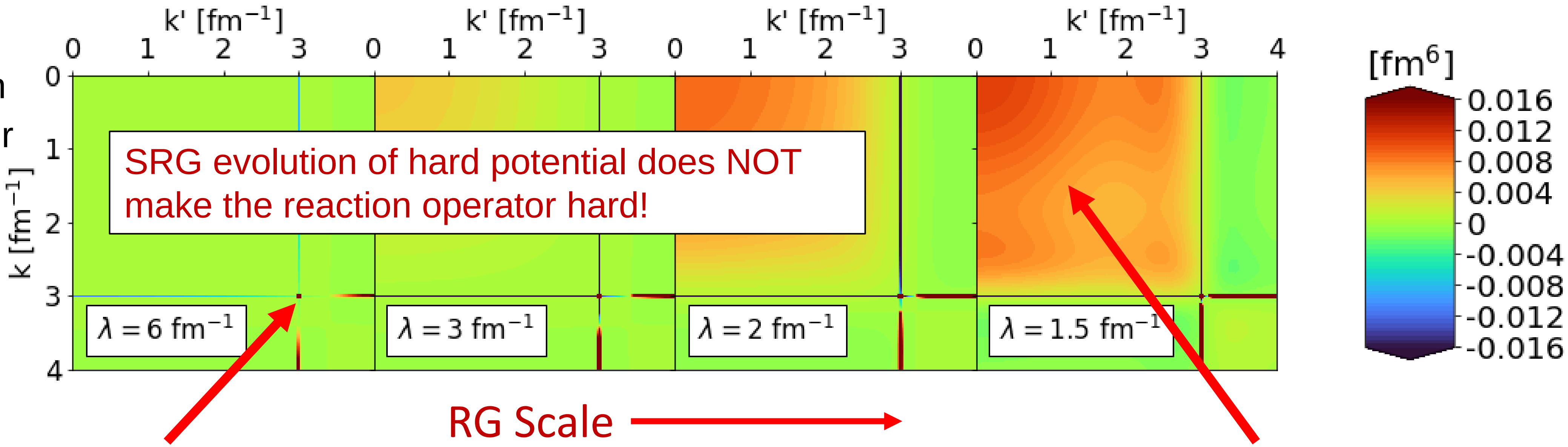

Bare operator is a discretized delta function in momentum space

$$\sim\delta(k-q)\delta(k'-q)$$

SRG evolution induces smooth, low-momentum contributions

Operator evolution

Fig. 3: Evolved momentum projection operator $U_\lambda a_q^\dagger a_q U_\lambda^\dagger$ for several λ values where $q = 3$ fm^{-1}.

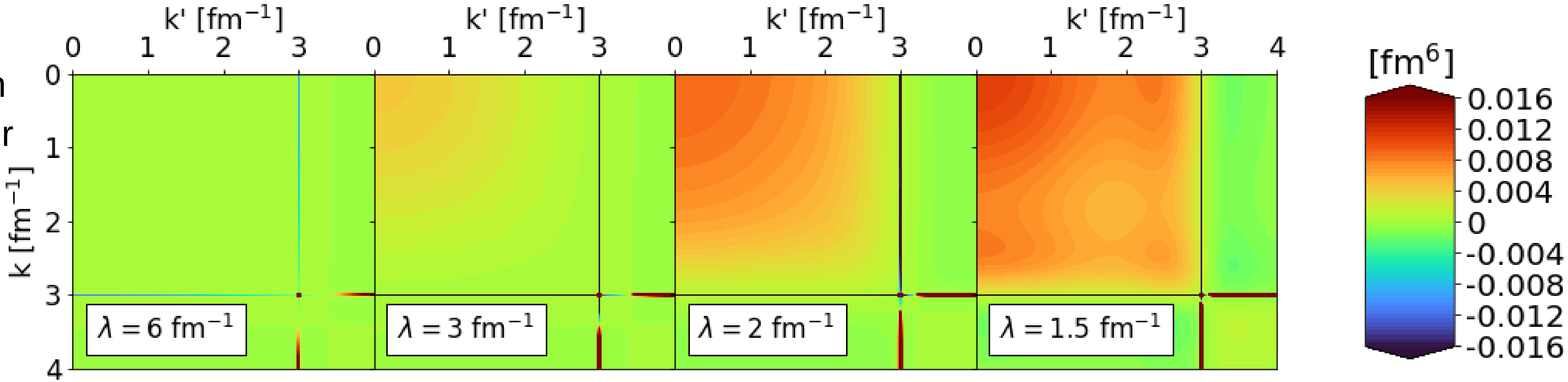

Fig. 4: Integrand of $\langle\psi_d^\lambda|U_\lambda a_q^\dagger a_q U_\lambda^\dagger|\psi_d^\lambda\rangle$ where $q = 3$ fm^{-1}.

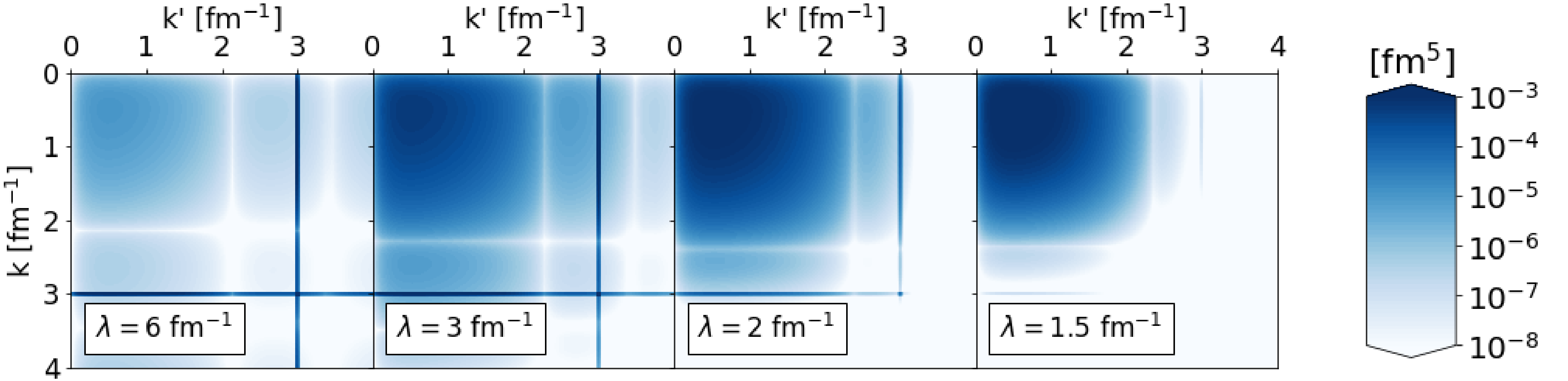

Operator evolution

- Each panel gives the correct expectation value from unitarity
- Expectation value is filtered to lower momentum at low RG resolution
- At high RG resolution $^3S_1$- $^3S_1$ channel contributes to ~25% of the expectation value $\langle \psi_d | a_q^\dagger a_q | \psi_d \rangle$ (heavy contribution from tensor force)

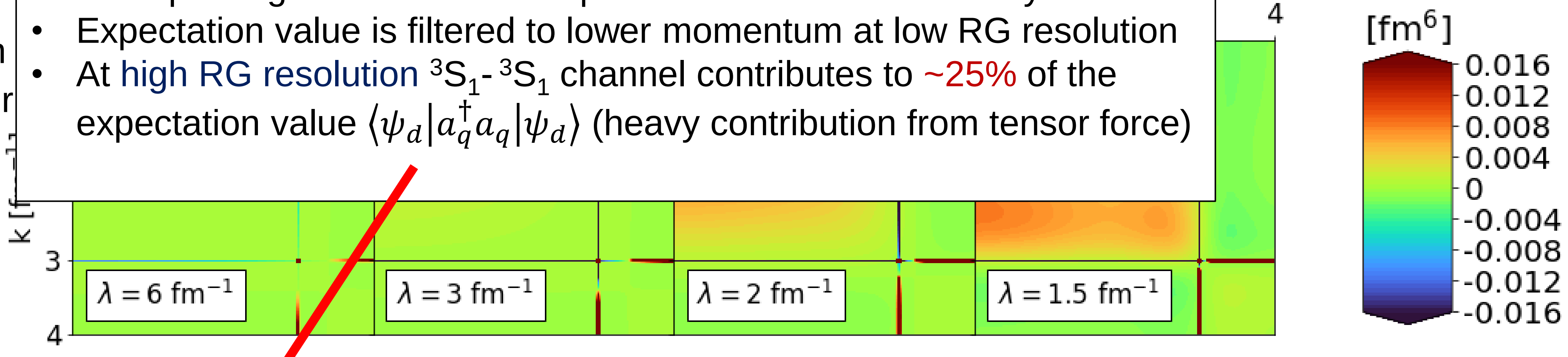

Fig. 3: Evolved momentum projection operator $U_\lambda a_q^\dagger a_q U_\lambda^\dagger$ for several λ values where $q = 3$ fm^{-1}.

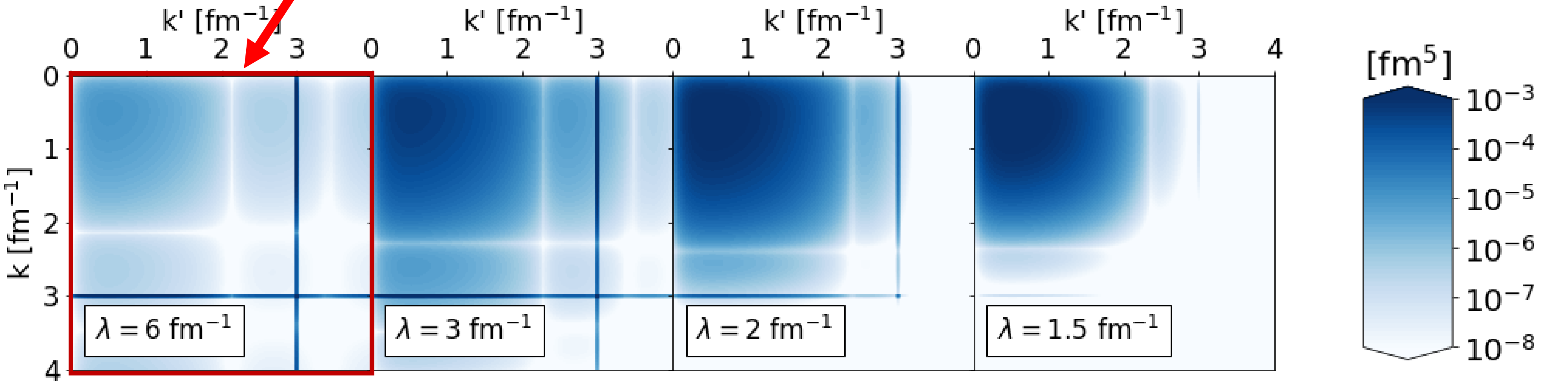

Fig. 4: Integrand of $\langle \psi_d^\lambda | U_\lambda a_q^\dagger a_q U_\lambda^\dagger | \psi_d^\lambda \rangle$ where $q = 3$ fm^{-1}.

Operator evolution

Fig. 3: Evolved momentum projection operator $U_\lambda a_q^\dagger a_q U_\lambda^\dagger$ for several λ values where $q = 3$ fm^{-1}.

- Each panel gives the correct expectation value from unitarity
- Expectation value is filtered to lower momentum at low RG resolution
- At high RG resolution $^3S_1$- $^3S_1$ channel contributes to ~25% of the expectation value $\langle \psi_d | a_q^\dagger a_q | \psi_d \rangle$ (heavy contribution from tensor force)
- At low RG resolution $^3S_1$- $^3S_1$ channel contributes to ~95% of the expectation value

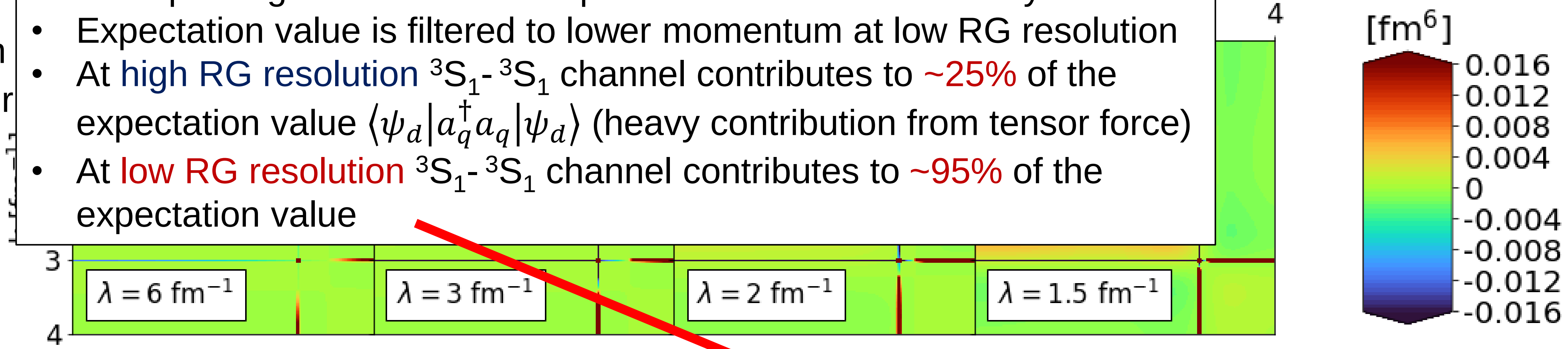

Fig. 4: Integrand of $\langle \psi_d^\lambda | U_\lambda a_q^\dagger a_q U_\lambda^\dagger | \psi_d^\lambda \rangle$ where $q = 3$ fm^{-1}.

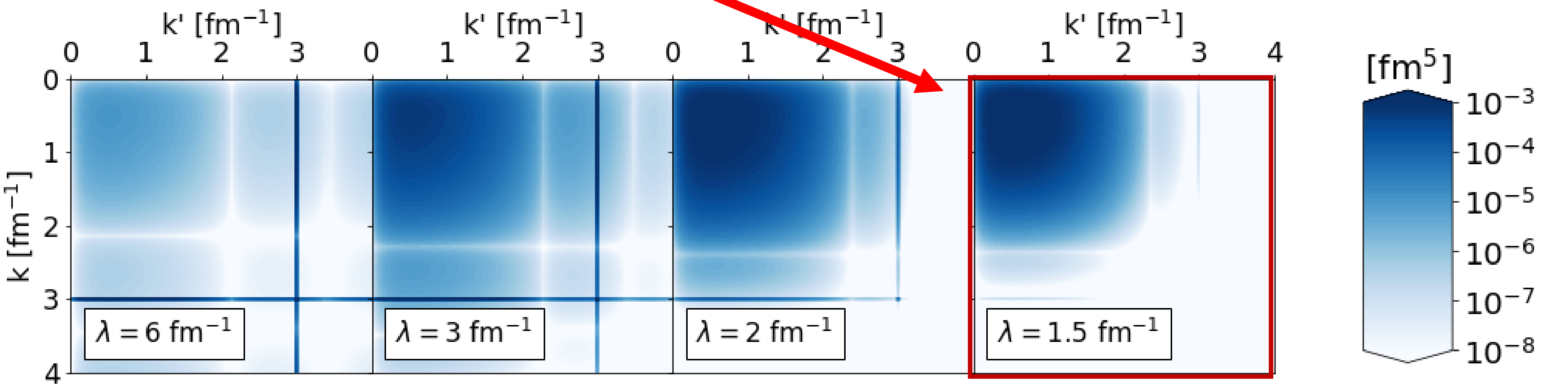

Momentum distributions at low RG resolution

- Apply SRG transformations to momentum distribution operators
  - Single-nucleon momentum distribution: $\hat{n}^{hi}(\boldsymbol{q}) = a^\dagger_{\boldsymbol{q}} a_{\boldsymbol{q}}$
  - Pair momentum distribution: $\hat{n}^{hi}(\boldsymbol{q}, \boldsymbol{Q}) = a^\dagger_{\frac{\boldsymbol{Q}}{2}+\boldsymbol{q}} a^\dagger_{\frac{\boldsymbol{Q}}{2}-\boldsymbol{q}} a_{\frac{\boldsymbol{Q}}{2}-\boldsymbol{q}} a_{\frac{\boldsymbol{Q}}{2}+\boldsymbol{q}}$

Momentum distributions at low RG resolution

- Apply SRG transformations to momentum distribution operators
  - Single-nucleon momentum distribution: $\hat{n}^{hi}(\boldsymbol{q}) = a^{\dagger}_{\boldsymbol{q}} a_{\boldsymbol{q}}$
  - Pair momentum distribution: $\hat{n}^{hi}(\boldsymbol{q}, \boldsymbol{Q}) = a^{\dagger}_{\frac{\boldsymbol{Q}}{2}+\boldsymbol{q}} a^{\dagger}_{\frac{\boldsymbol{Q}}{2}-\boldsymbol{q}} a_{\frac{\boldsymbol{Q}}{2}-\boldsymbol{q}} a_{\frac{\boldsymbol{Q}}{2}+\boldsymbol{q}}$
- Expand SRG transformation to 2-body level

$$\widehat{U}_{\lambda} = 1 + \frac{1}{4} \sum_{\boldsymbol{K},\boldsymbol{k},\boldsymbol{k}'} \delta U^{(2)}_{\lambda}(\boldsymbol{k}, \boldsymbol{k}') a^{\dagger}_{\frac{\boldsymbol{K}}{2}+\boldsymbol{k}} a^{\dagger}_{\frac{\boldsymbol{K}}{2}-\boldsymbol{k}} a_{\frac{\boldsymbol{K}}{2}-\boldsymbol{k}'} a_{\frac{\boldsymbol{K}}{2}+\boldsymbol{k}'} + \cdots$$

- $\delta U^{(2)}_{\lambda}$ term is fixed by SRG evolution on $A = 2$ and inherits the symmetries of V_{NN}

Momentum distributions at low RG resolution

- Apply SRG transformations to momentum distribution operators
  - Single-nucleon momentum distribution: $\hat{n}^{hi}(\boldsymbol{q}) = a_{\boldsymbol{q}}^{\dagger} a_{\boldsymbol{q}}$
  - Pair momentum distribution: $\hat{n}^{hi}(\boldsymbol{q},\boldsymbol{Q}) = a_{\frac{\boldsymbol{Q}}{2}+\boldsymbol{q}}^{\dagger} a_{\frac{\boldsymbol{Q}}{2}-\boldsymbol{q}}^{\dagger} a_{\frac{\boldsymbol{Q}}{2}-\boldsymbol{q}} a_{\frac{\boldsymbol{Q}}{2}+\boldsymbol{q}}$
- Expand SRG transformation to 2-body level

$$\widehat{U}_{\lambda} = 1 + \frac{1}{4} \sum_{\boldsymbol{K},\boldsymbol{k},\boldsymbol{k'}} \delta U_{\lambda}^{(2)}(\boldsymbol{k},\boldsymbol{k}') a_{\frac{\boldsymbol{K}}{2}+\boldsymbol{k}}^{\dagger} a_{\frac{\boldsymbol{K}}{2}-\boldsymbol{k}}^{\dagger} a_{\frac{\boldsymbol{K}}{2}-\boldsymbol{k}'} a_{\frac{\boldsymbol{K}}{2}+\boldsymbol{k}'} + \cdots$$

- $\delta U_{\lambda}^{(2)}$ term is fixed by SRG evolution on $A = 2$ and inherits the symmetries of V_{NN}
- **Strategy**: Apply Wick's theorem to evaluate $\widehat{U}_{\lambda}\hat{n}^{hi}(\boldsymbol{q})\widehat{U}_{\boldsymbol{\lambda}}^{\dagger}$ and $\widehat{U}_{\lambda}\hat{n}^{hi}(\boldsymbol{q},\boldsymbol{Q})\widehat{U}_{\boldsymbol{\lambda}}^{\dagger}$ truncating 3-body and higher terms

Momentum distributions at low RG resolution

- **Example**: Evolved single-nucleon momentum distribution

$$\widehat{U}_\lambda \hat{n}^{hi}(\boldsymbol{q}) \widehat{U}_{\boldsymbol{\lambda}}^\dagger$$
$$\approx a_{\boldsymbol{q}}^\dagger a_{\boldsymbol{q}} + \frac{1}{2} \sum_{\boldsymbol{K},\boldsymbol{k}} [\delta U_\lambda^{(2)}\left(\boldsymbol{k}, \boldsymbol{q} - \frac{\boldsymbol{K}}{2}\right) a_{\frac{\boldsymbol{K}}{2}+\boldsymbol{k}}^\dagger a_{\frac{\boldsymbol{K}}{2}-\boldsymbol{k}}^\dagger a_{\boldsymbol{K}-\boldsymbol{q}} a_{\boldsymbol{q}} + \delta U_\lambda^{\dagger(2)}\left(\boldsymbol{q} - \frac{\boldsymbol{K}}{2}, \boldsymbol{k}\right) a_{\boldsymbol{q}}^\dagger a_{\boldsymbol{K}-\boldsymbol{q}}^\dagger a_{\frac{\boldsymbol{K}}{2}-\boldsymbol{k}} a_{\frac{\boldsymbol{K}}{2}+\boldsymbol{k}}]$$
$$+ \frac{1}{4} \sum_{\boldsymbol{K},\boldsymbol{k},\boldsymbol{k}'} \delta U_\lambda^{(2)}\left(\boldsymbol{k}, \boldsymbol{q} - \frac{\boldsymbol{K}}{2}\right) \delta U_\lambda^{\dagger(2)}\left(\boldsymbol{q} - \frac{\boldsymbol{K}}{2}, \boldsymbol{k}'\right) a_{\frac{\boldsymbol{K}}{2}+\boldsymbol{k}}^\dagger a_{\frac{\boldsymbol{K}}{2}-\boldsymbol{k}}^\dagger a_{\frac{\boldsymbol{K}}{2}-\boldsymbol{k}'} a_{\frac{\boldsymbol{K}}{2}+\boldsymbol{k}'}$$

- For operator that probes high momentum ($q \gg \lambda$), the low RG resolution wave function filters out first few terms leaving only $\delta U \delta U^\dagger$ term

Momentum distributions at low RG resolution

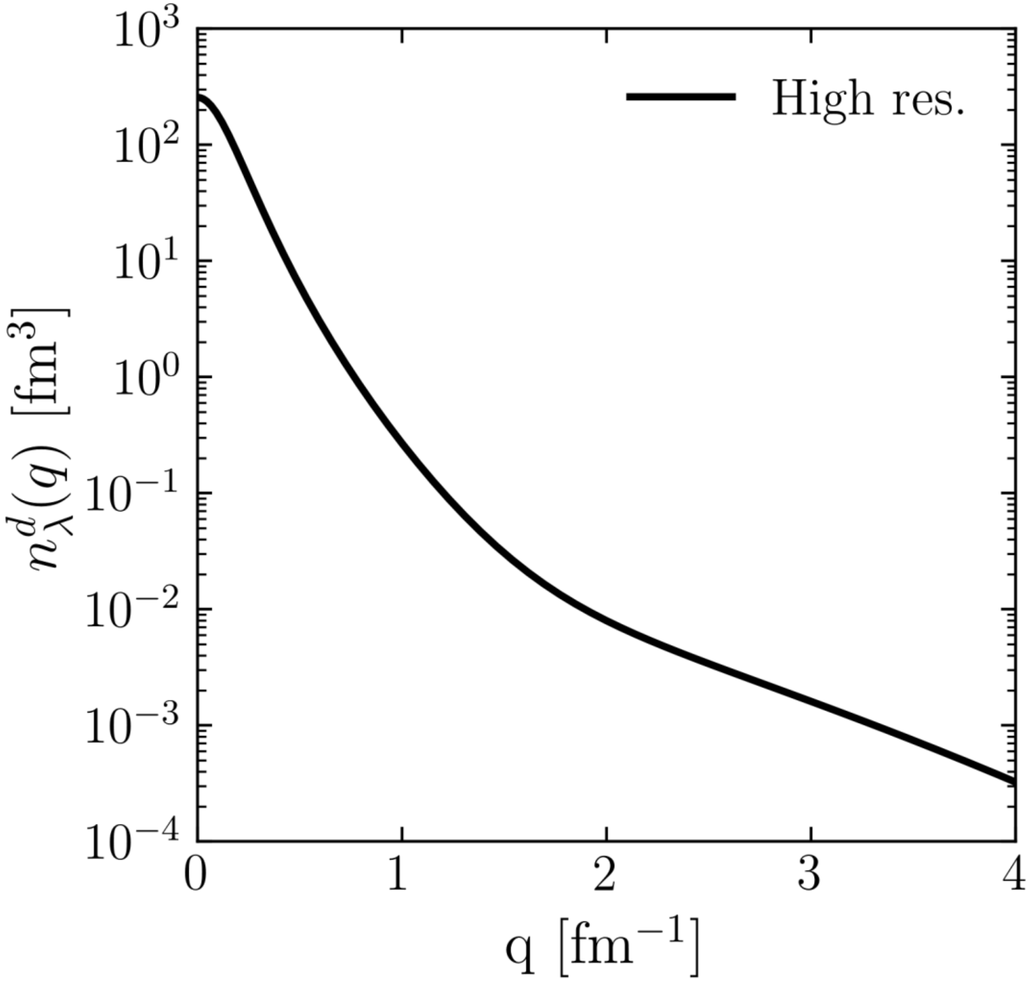

Fig. 5: Contributions to deuteron momentum distribution with AV18 and $\lambda = 1.35$ fm^{-1}.

- Deuteron example

$$n^{lo}(\boldsymbol{q}) = (1 + \delta U) a^\dagger_{\boldsymbol{q}} a_{\boldsymbol{q}} (1 + \delta U^\dagger)$$

$$\langle \psi_d^{hi} | a^\dagger_{\boldsymbol{q}} a_{\boldsymbol{q}} | \psi_d^{hi} \rangle$$

Momentum distributions at low RG resolution

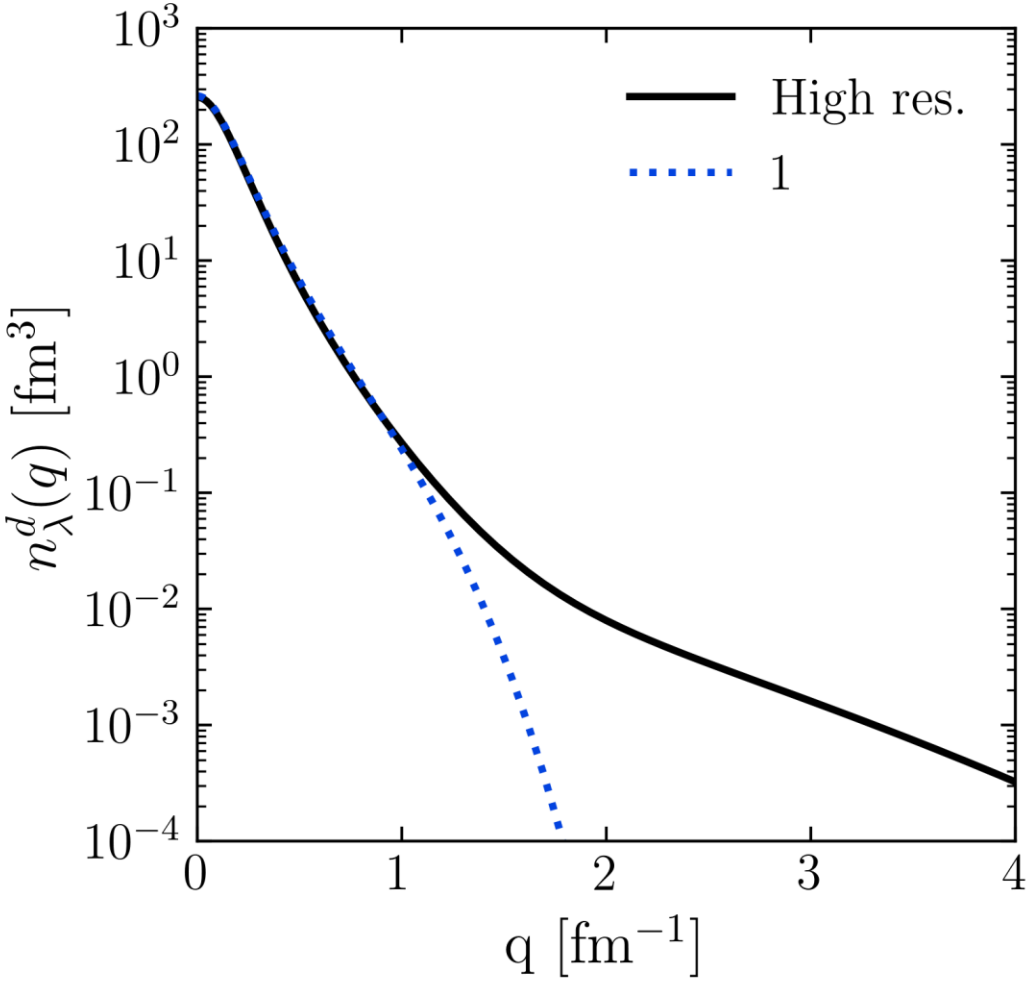

Fig. 5: Contributions to deuteron momentum distribution with AV18 and $\lambda = 1.35$ fm^{-1}.

- Deuteron example

$$n^{lo}(\boldsymbol{q}) = (1 + \delta U) a_{\boldsymbol{q}}^\dagger a_{\boldsymbol{q}} (1 + \delta U^\dagger)$$

$$\langle \psi_d^{hi} | a_{\boldsymbol{q}}^\dagger a_{\boldsymbol{q}} | \psi_d^{hi} \rangle$$

$$\langle \psi_d^{lo} | a_{\boldsymbol{q}}^\dagger a_{\boldsymbol{q}} | \psi_d^{lo} \rangle$$

Momentum distributions at low RG resolution

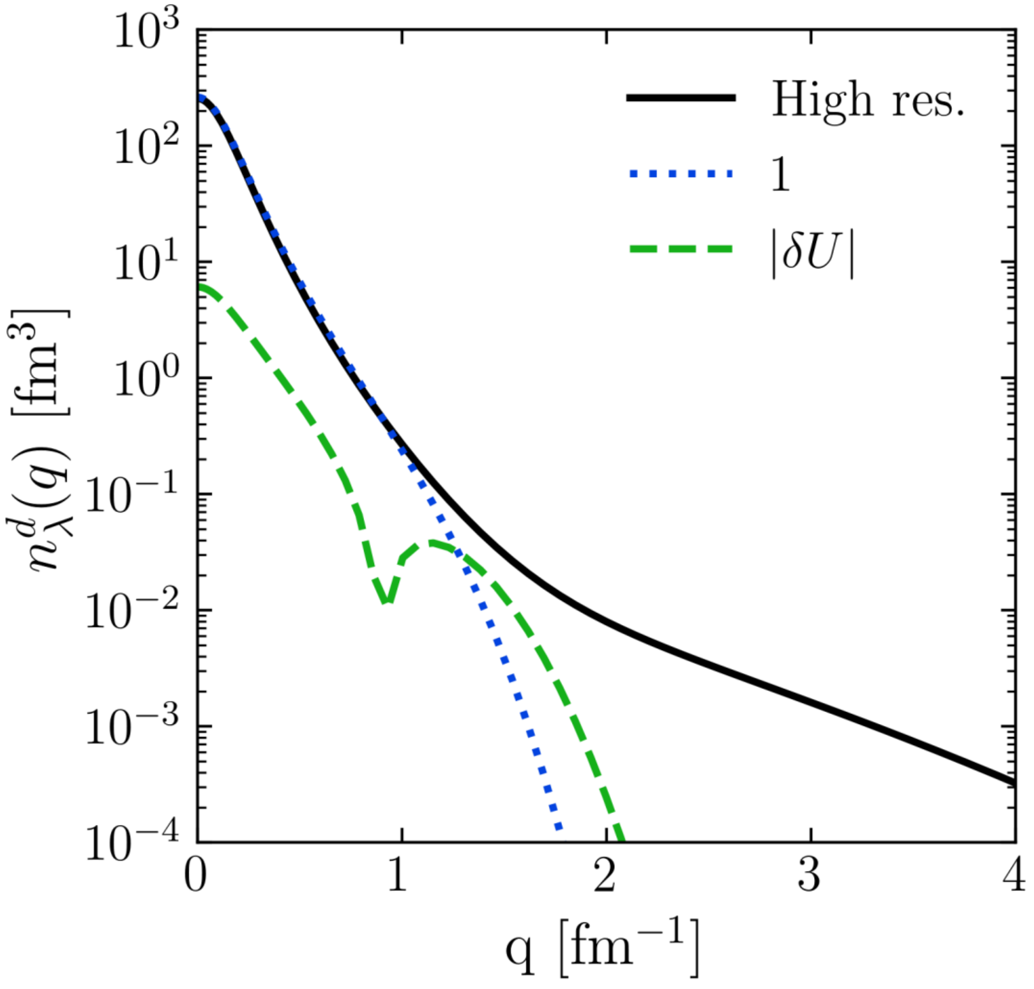

Fig. 5: Contributions to deuteron momentum distribution with AV18 and $\lambda = 1.35$ fm^{-1}.

- Deuteron example

$$n^{lo}(\boldsymbol{q}) = (1 + \delta U) a^\dagger_{\boldsymbol{q}} a_{\boldsymbol{q}} (1 + \delta U^\dagger)$$

$$\langle \psi_d^{hi} | a^\dagger_{\boldsymbol{q}} a_{\boldsymbol{q}} | \psi_d^{hi} \rangle$$

$$\langle \psi_d^{lo} | a^\dagger_{\boldsymbol{q}} a_{\boldsymbol{q}} | \psi_d^{lo} \rangle$$

$$\langle \psi_d^{lo} | \delta U a^\dagger_{\boldsymbol{q}} a_{\boldsymbol{q}} + a^\dagger_{\boldsymbol{q}} a_{\boldsymbol{q}} \delta U^\dagger | \psi_d^{lo} \rangle$$

Momentum distributions at low RG resolution

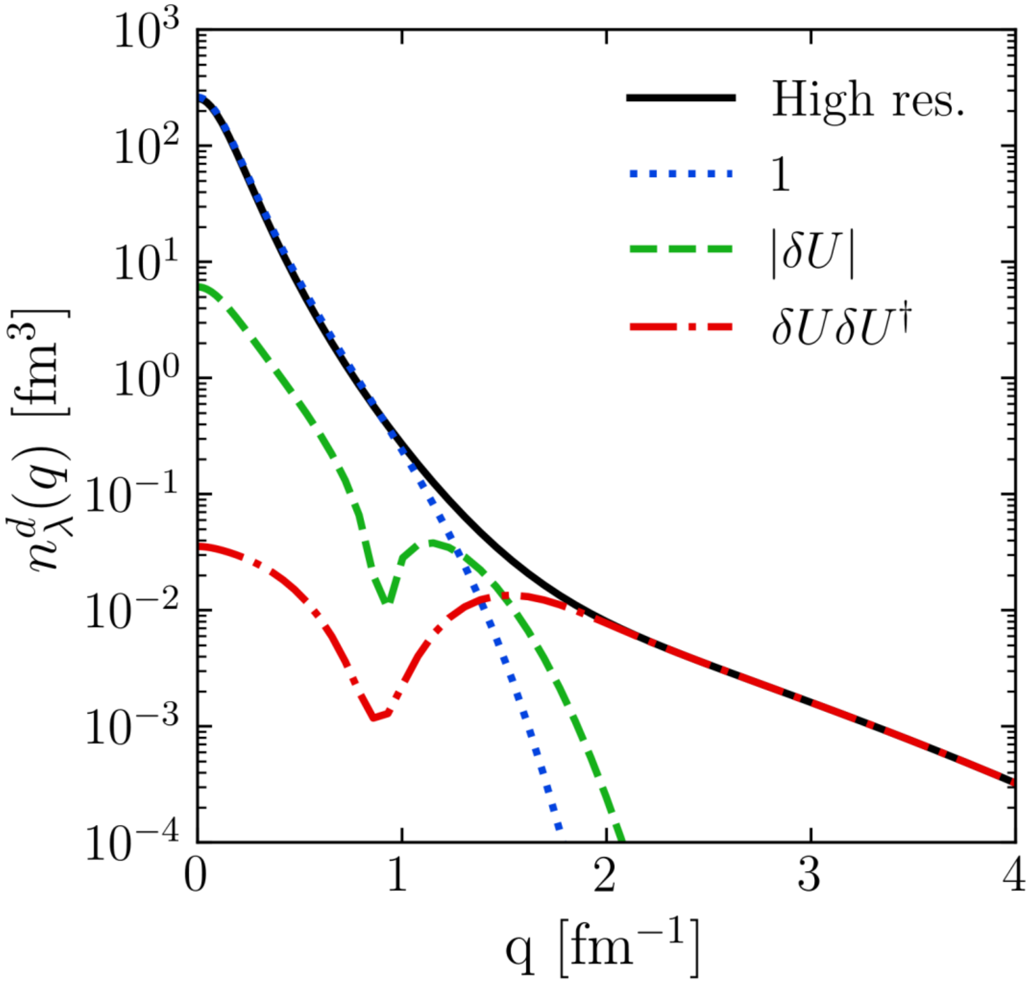

Fig. 5: Contributions to deuteron momentum distribution with AV18 and $\lambda = 1.35$ fm^{-1}.

- Deuteron example

$$n^{lo}(\boldsymbol{q}) = (1 + \delta U) a^\dagger_{\boldsymbol{q}} a_{\boldsymbol{q}} (1 + \delta U^\dagger)$$

$$\langle \psi_d^{hi} | a^\dagger_{\boldsymbol{q}} a_{\boldsymbol{q}} | \psi_d^{hi} \rangle$$

$$\langle \psi_d^{lo} | a^\dagger_{\boldsymbol{q}} a_{\boldsymbol{q}} | \psi_d^{lo} \rangle$$

$$\langle \psi_d^{lo} | \delta U a^\dagger_{\boldsymbol{q}} a_{\boldsymbol{q}} + a^\dagger_{\boldsymbol{q}} a_{\boldsymbol{q}} \delta U^\dagger | \psi_d^{lo} \rangle$$

$$\langle \psi_d^{lo} | \delta U a^\dagger_{\boldsymbol{q}} a_{\boldsymbol{q}} \delta U^\dagger | \psi_d^{lo} \rangle$$

Momentum distributions at low RG resolution

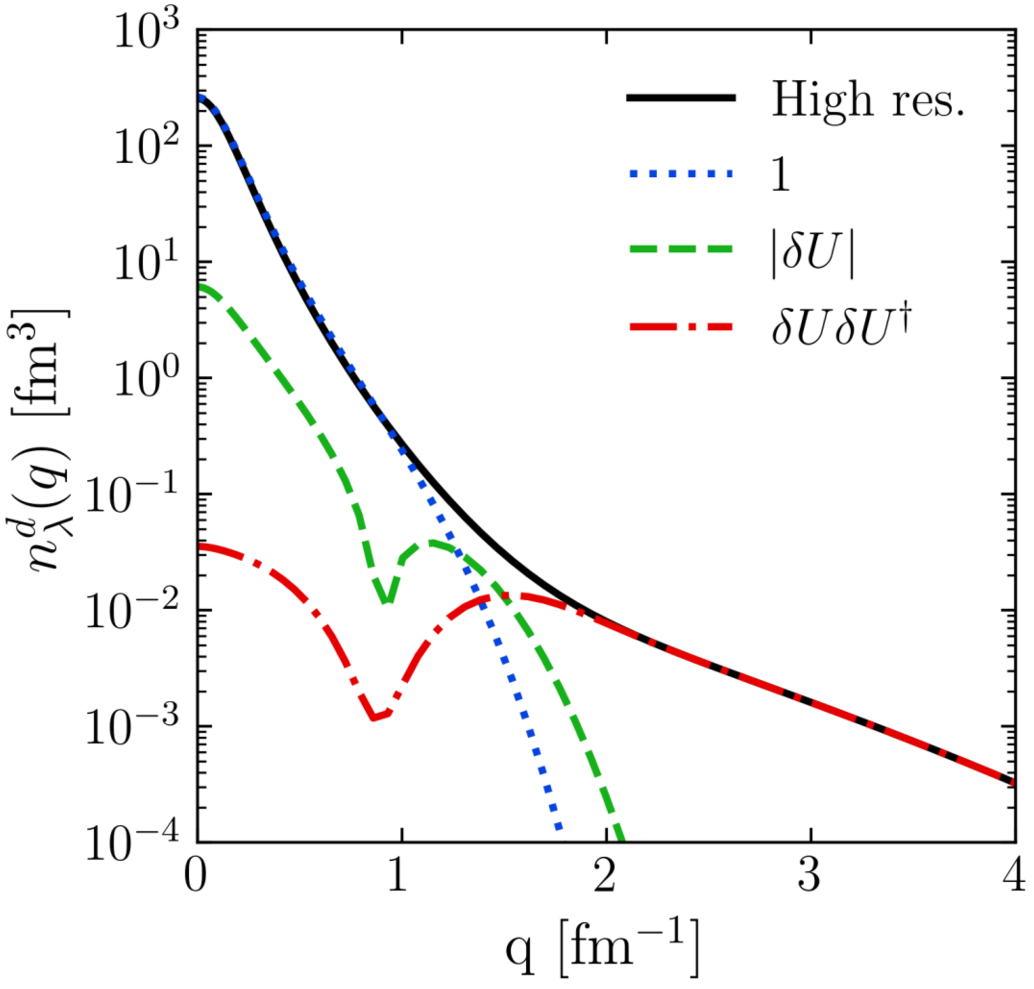

Fig. 5: Contributions to deuteron momentum distribution with AV18 and $\lambda = 1.35$ fm^{-1}.

- For high-q, the $\delta U_\lambda \delta U_\lambda^\dagger$ 2-body term dominates

$$\approx \sum_{\boldsymbol{K},\boldsymbol{k},\boldsymbol{k}'}^{\lambda} \delta U_\lambda(\boldsymbol{k},\boldsymbol{q}) \delta U_\lambda^\dagger(\boldsymbol{q},\boldsymbol{k}') a^\dagger_{\frac{\boldsymbol{K}}{2}+\boldsymbol{k}} a^\dagger_{\frac{\boldsymbol{K}}{2}-\boldsymbol{k}} a_{\frac{\boldsymbol{K}}{2}-\boldsymbol{k}'} a_{\frac{\boldsymbol{K}}{2}+\boldsymbol{k}'}$$

Momentum distributions at low RG resolution

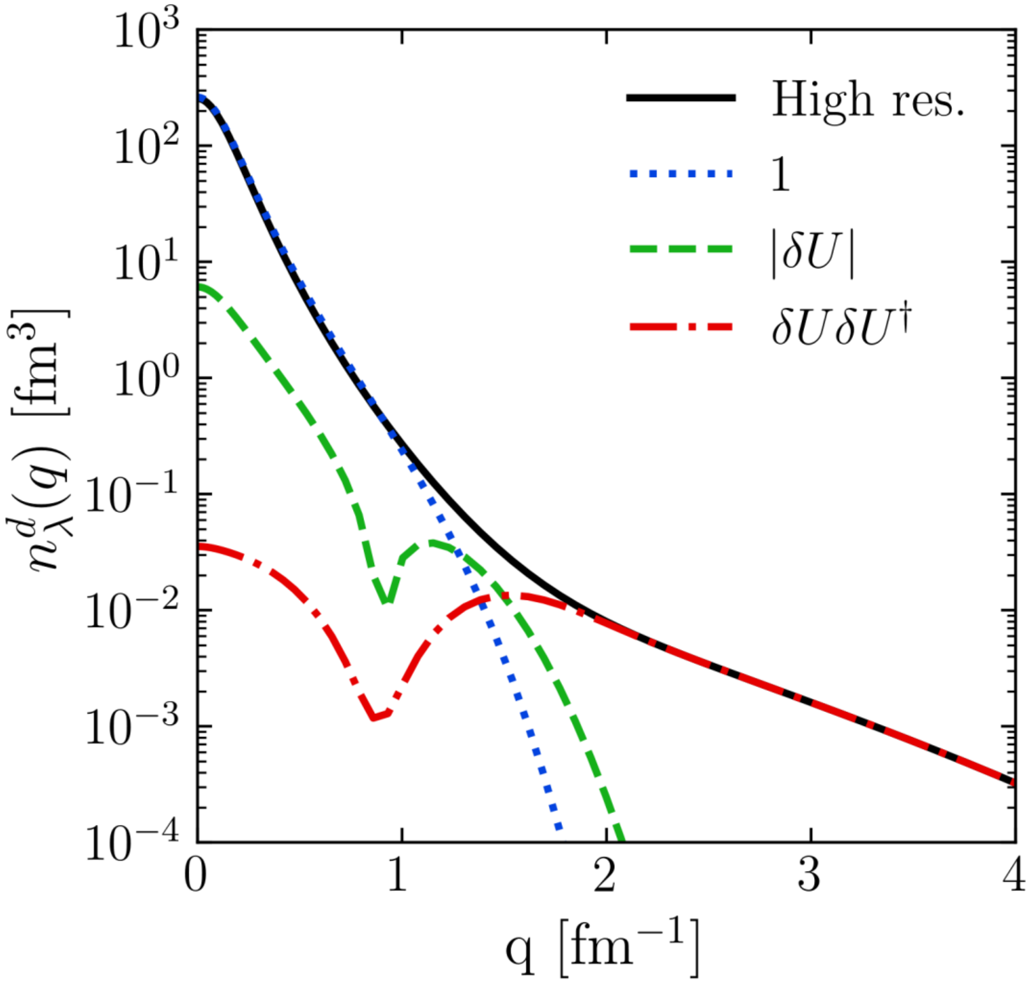

Fig. 5: Contributions to deuteron momentum distribution with AV18 and $\lambda = 1.35$ fm^{-1}.

- For high-q, the $\delta U_\lambda \delta U_\lambda^\dagger$ 2-body term dominates

$$\approx \sum_{\boldsymbol{K},\boldsymbol{k},\boldsymbol{k}'}^{\lambda} \delta U_\lambda(\boldsymbol{k},\boldsymbol{q}) \delta U_\lambda^\dagger(\boldsymbol{q},\boldsymbol{k}') a^\dagger_{\frac{\boldsymbol{K}}{2}+\boldsymbol{k}} a^\dagger_{\frac{\boldsymbol{K}}{2}-\boldsymbol{k}} a_{\frac{\boldsymbol{K}}{2}-\boldsymbol{k}'} a_{\frac{\boldsymbol{K}}{2}+\boldsymbol{k}'}$$

$\downarrow$

Factorization: $\delta U_\lambda(\boldsymbol{k},\boldsymbol{q}) \approx F_\lambda^{lo}(\boldsymbol{k}) F_\lambda^{hi}(\boldsymbol{q})$

$\downarrow$

$$\approx \left|F_\lambda^{hi}(\boldsymbol{q})\right|^2 \sum_{\boldsymbol{K},\boldsymbol{k},\boldsymbol{k}'}^{\lambda} F_\lambda^{lo}(\boldsymbol{k}) F_\lambda^{lo}(\boldsymbol{k}') a^\dagger_{\frac{\boldsymbol{K}}{2}+\boldsymbol{k}} a^\dagger_{\frac{\boldsymbol{K}}{2}-\boldsymbol{k}} a_{\frac{\boldsymbol{K}}{2}-\boldsymbol{k}'} a_{\frac{\boldsymbol{K}}{2}+\boldsymbol{k}'}$$

Factorization

- Factorization of SRG transformations imply scaling of high-q tails
- Consider ratio $\frac{n^A(\boldsymbol{q})}{n^d(\boldsymbol{q})}$ for $q \gg \lambda$,

$$\frac{\langle \Psi_\lambda^A | U_\lambda a_q^\dagger a_q U_\lambda^\dagger | \Psi_\lambda^A \rangle}{\langle \Psi_\lambda^d | U_\lambda a_q^\dagger a_q U_\lambda^\dagger | \Psi_\lambda^d \rangle} = \cancel{\frac{\left| F_\lambda^{hi}(\boldsymbol{q}) \right|^2}{\left| F_\lambda^{hi}(\boldsymbol{q}) \right|^2}} \times \frac{\left\langle \Psi_\lambda^A \middle| \sum_{\boldsymbol{K},\boldsymbol{k},\boldsymbol{k}'}^{\lambda} F_\lambda^{lo}(\boldsymbol{k}) F_\lambda^{lo}(\boldsymbol{k}') a_{\frac{\boldsymbol{K}}{2}+\boldsymbol{k}}^\dagger a_{\frac{\boldsymbol{K}}{2}-\boldsymbol{k}}^\dagger a_{\frac{\boldsymbol{K}}{2}-\boldsymbol{k}'} a_{\frac{\boldsymbol{K}}{2}+\boldsymbol{k}'} \middle| \Psi_\lambda^A \right\rangle}{\left\langle \Psi_\lambda^d \middle| \sum_{\boldsymbol{K},\boldsymbol{k},\boldsymbol{k}'}^{\lambda} F_\lambda^{lo}(\boldsymbol{k}) F_\lambda^{lo}(\boldsymbol{k}') a_{\frac{\boldsymbol{K}}{2}+\boldsymbol{k}}^\dagger a_{\frac{\boldsymbol{K}}{2}-\boldsymbol{k}}^\dagger a_{\frac{\boldsymbol{K}}{2}-\boldsymbol{k}'} a_{\frac{\boldsymbol{K}}{2}+\boldsymbol{k}'} \middle| \Psi_\lambda^d \right\rangle}$$

- High-q dependence cancels leaving ratio only sensitive to low-momentum physics

Why low RG resolution?

- Methods that rely on soft interactions work well!

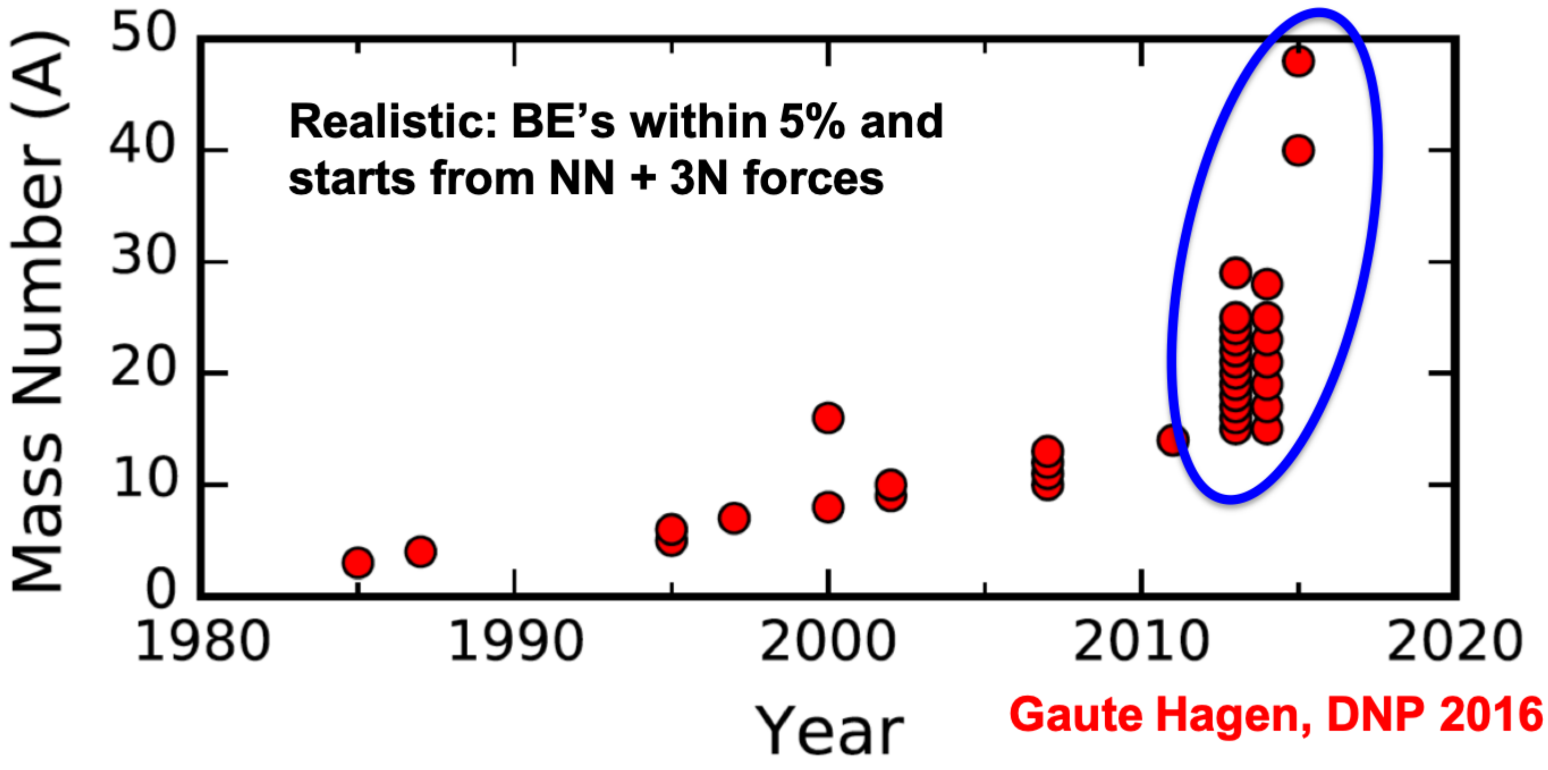

Why low RG resolution?

- Methods that rely on soft interactions work well!
- What SRC physics can we describe using simple approximations?
- Try Hartree-Fock with a local density approximation to evaluate nuclear matrix elements

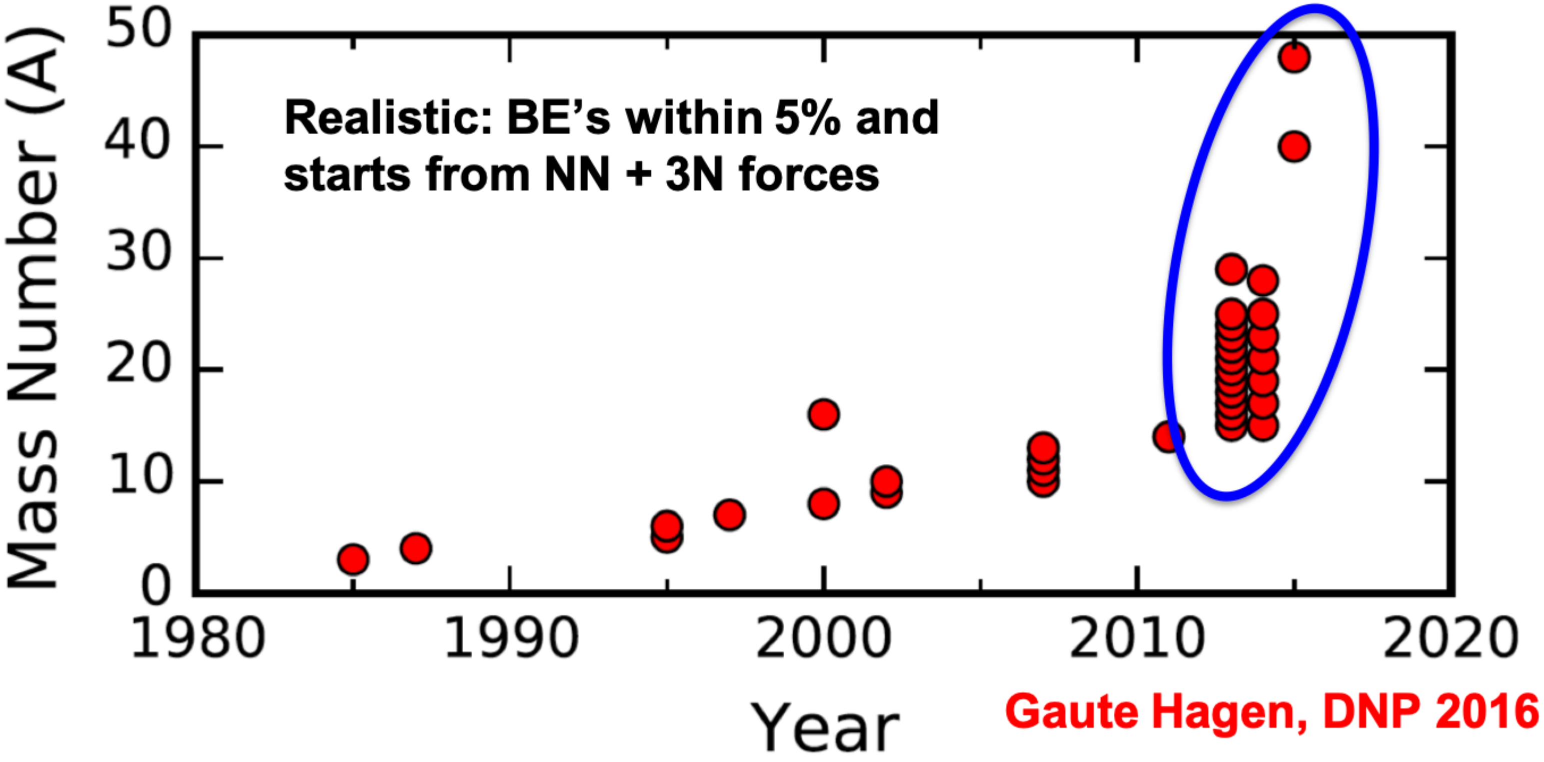

Gaute Hagen, DNP 2016

[1] R.B. Wiringa et al., Phys. Rev. C **89**, 024305 (2014)
https://www.phy.anl.gov/theory/research/momenta/
[2] K. Bennaceur et al., Comput. Phys. Commun. **168**, 96 (2005)

Proton momentum distributions

- Low RG resolution calculations reproduce momentum distributions of AV18 QMC calculations[1] (high RG resolution)

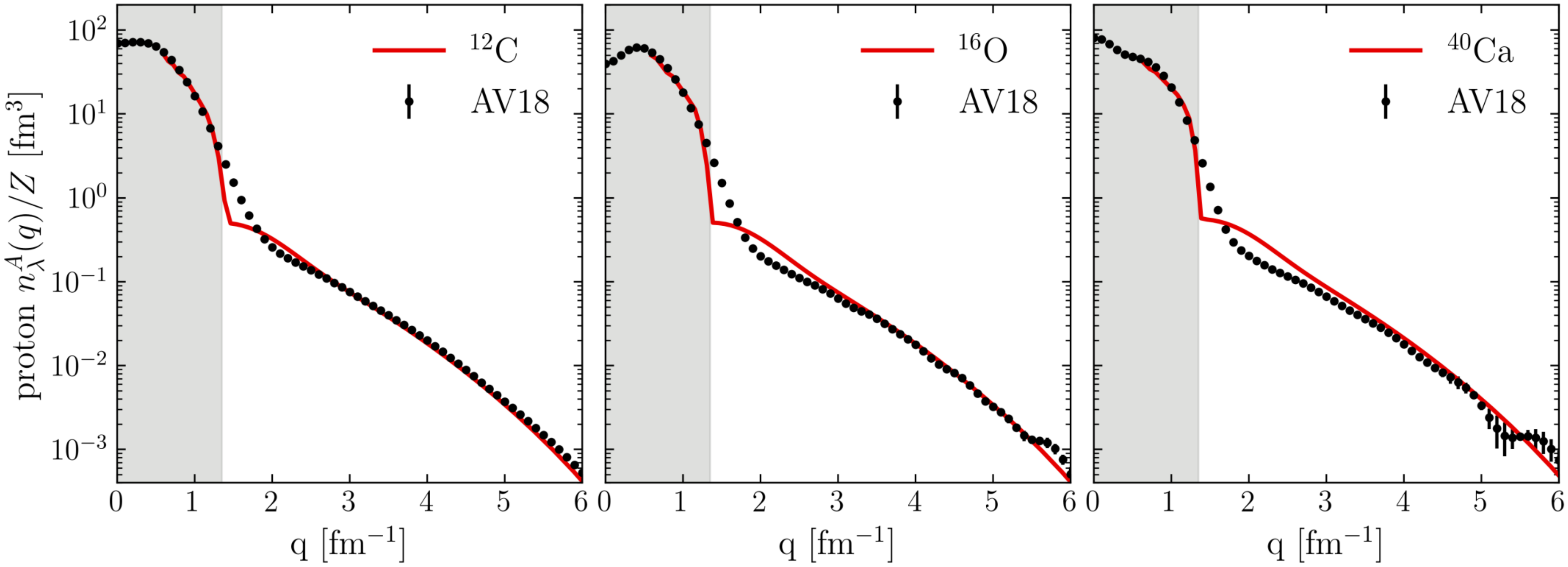

Fig. 6: Proton momentum distributions for ^{12}C, ^{16}O, and ^{40}Ca under HF+LDA with AV18, $\lambda = 1.35$ fm^{-1}, and densities from Skyrme EDF SLy4 using the HFBRAD code[2].

[1]R.B. Wiringa et al., Phys. Rev. C **89**, 024305 (2014)
https://www.phy.anl.gov/theory/research/momenta/
[2]K. Bennaceur et al., Comput. Phys. Commun. **168**, 96 (2005)

Proton momentum distributions

- Low RG resolution calculations reproduce momentum distributions of AV18 QMC calculations[1] (high RG resolution)

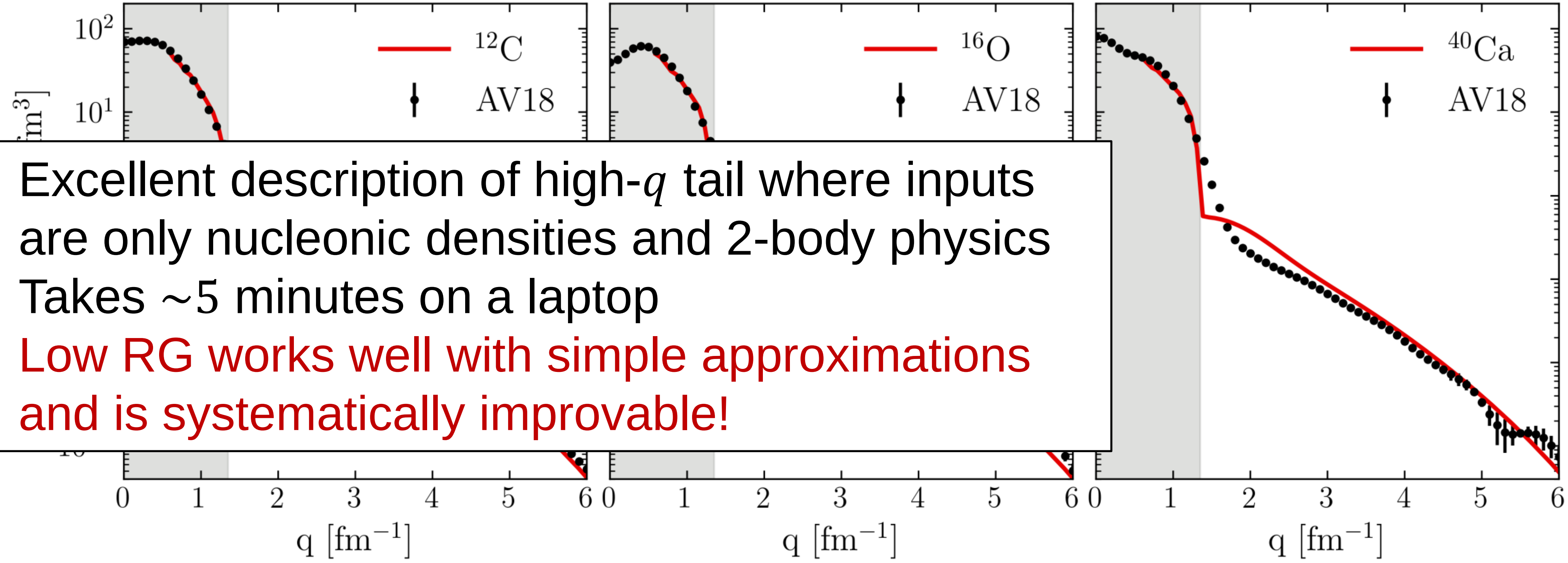

- Excellent description of high-q tail where inputs are only nucleonic densities and 2-body physics
- Takes ~5 minutes on a laptop
- Low RG works well with simple approximations and is systematically improvable!

Fig. 6: Proton momentum distributions for ^{12}C, ^{16}O, and ^{40}Ca under HF+LDA with AV18, λ = 1.35 fm^{-1}, and densities from Skyrme EDF SLy4 using the HFBRAD code[2].

Proton momentum distributions

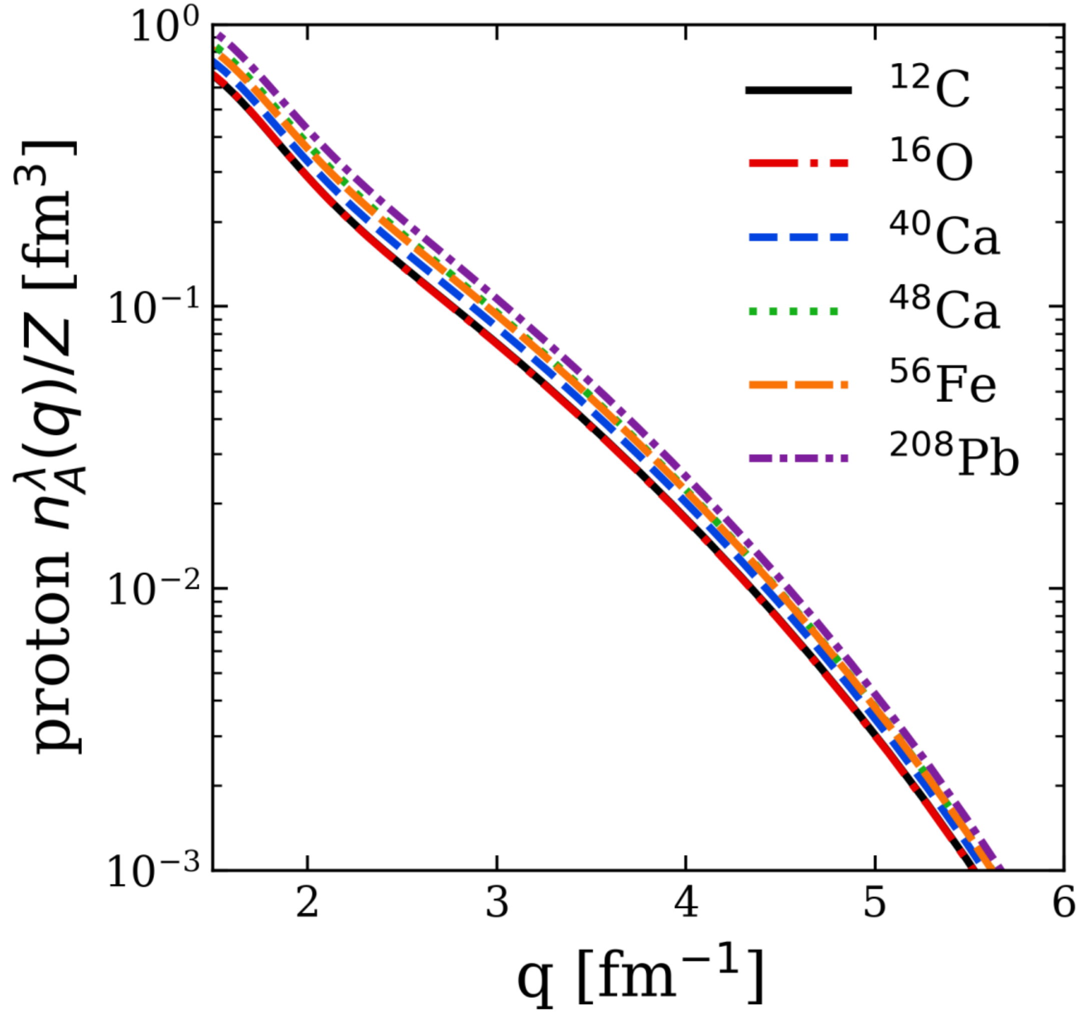

Fig. 7: Proton momentum distributions under HF+LDA with AV18 and $\lambda = 1.35$ fm^{-1}, showing several nuclei.

- Universality: High-q dependence from universal function $\approx \left|F_\lambda^{hi}(q)\right|^2$ fixed by 2-body and insensitive to nucleus

SRC scaling factors

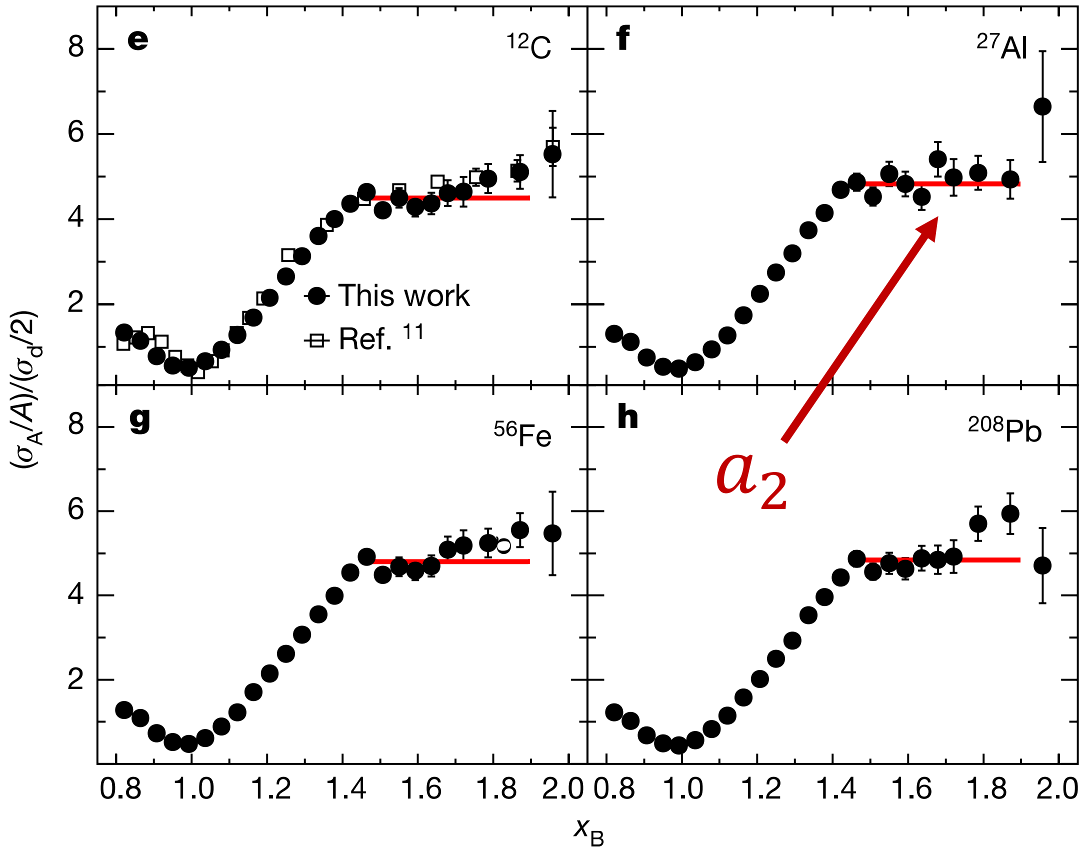

Fig. 8: Ratio of per-nucleon electron scattering cross section of nucleus A to that of deuterium, where the red line indicates a constant fit. Figure from B. Schmookler et al. (CLAS), Nature **566**, 354 (2019).

- SRC scaling factors a_2 defined by plateau in cross section ratio $\frac{2\sigma_A}{A\sigma_d}$ at $1.45 \leq x \leq 1.9$
- Closely related to the ratio of bound-nucleon probability distributions in the limits of vanishing relative distance (infinitely high relative momentum)
- Extract a_2 from momentum distributions

$$a_2 = \lim_{q\to\infty} \frac{P^A(q)}{P^d(q)} \approx \frac{\int_{\Delta q^{high}} dq P^A(q)}{\int_{\Delta q^{high}} dq P^d(q)}$$

where $P^A(q)$ is the single-nucleon probability distribution in nucleus A

[1]E. Chabanat et al., Nucl. Phys. A **635**, 231 (1998)
[2]J. Decharge et al., Phys. Rev. C **21**, 1568 (1980)
[3]B. Schmookler et al. (CLAS), Nature **566**, 354 (2019)
[4]J. Ryckebusch et al., Phys. Rev. C **100**, 054620 (2019)

SRC scaling factors

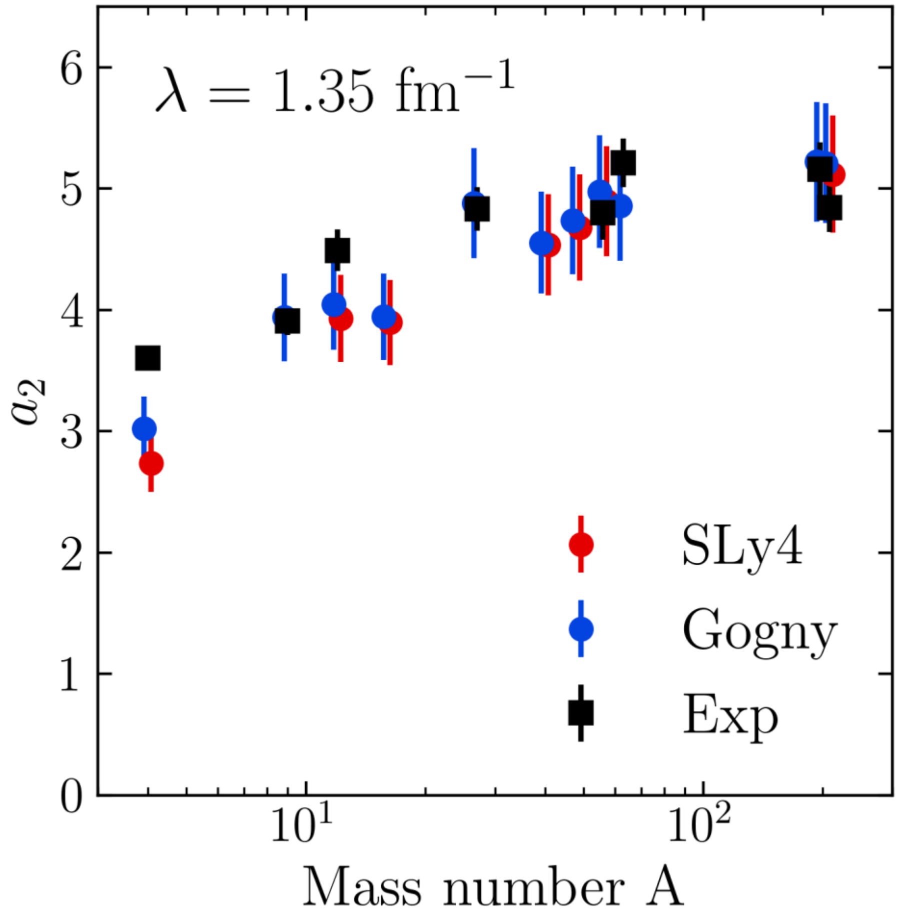

Fig. 9: a_2 scale factors using single-nucleon momentum distributions under HF+LDA (SLy4 in red[1], Gogny[2] in blue) with AV18 and $\lambda = 1.35$ fm^{-1} compared to experimental values[3].

$$a_2 = \lim_{q\to\infty} \frac{P^A(q)}{P^d(q)} \approx \frac{\int_{\Delta q^{high}} dq P^A(q)}{\int_{\Delta q^{high}} dq P^d(q)}$$

- High momentum behavior is characterized by 2-body $\left|F_\lambda^{hi}(q)\right|^2$ which cancels leaving ratio of mean-field (low-k) physics
- Good agreement with a_2 values from experiment[3] and LCA calculations[4] using two different EDFs
- Error bars from varying Δq^{high}

SRC phenomenology

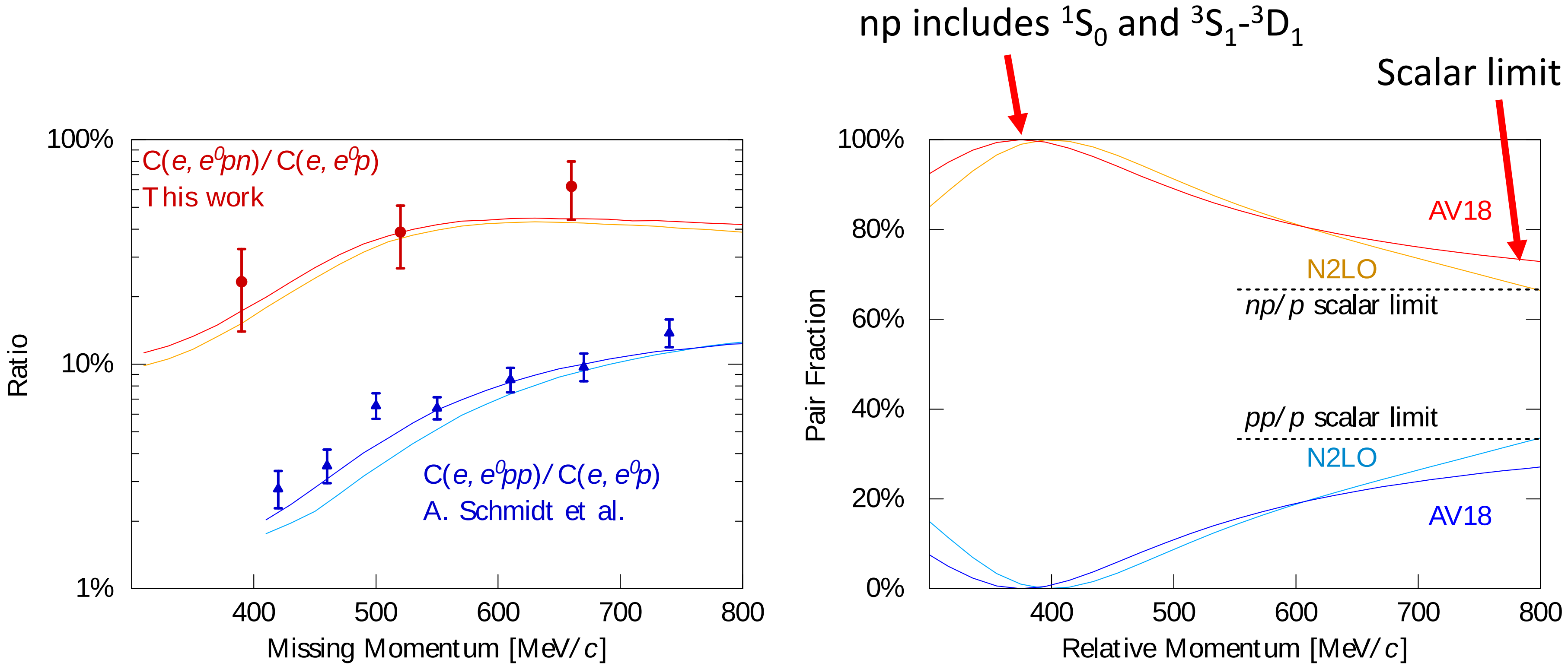

Fig. 10: (a) Ratio of two-nucleon to single-nucleon electron-scattering cross sections for carbon as a function of missing momentum. (b) Fraction of np to p and pp to p pairs versus the relative momentum. Figure from CLAS collaboration publication[1].

- At high RG resolution, the tensor force and the repulsive core of the NN interaction kicks nucleon pairs into SRCs
- np dominates because the tensor force requires spin triplet pairs, whereas pp are spin singlets
- Do we describe this physics at low RG resolution?

[1] I. Korover et al. (CLAS), arXiv:2004.07304 (2014)

SRC phenomenology

- At low RG resolution, SRCs are suppressed in the wave function and shifted into the operator

$$\hat{n}^{lo}(\boldsymbol{q}) = \hat{U}_\lambda a^\dagger_{\boldsymbol{q}} a_{\boldsymbol{q}} \hat{U}^\dagger_\lambda = U_\lambda(\boldsymbol{k}, \boldsymbol{q}) U^\dagger_\lambda(\boldsymbol{q}, \boldsymbol{k}')$$

- Take ratio of $^3S_1$ and $^1S_0$ SRG transformations fixing low-momenta to $k_0 = 0.1$ fm^{-1}
- This physics is established in the 2-body system – can apply to any nucleus!

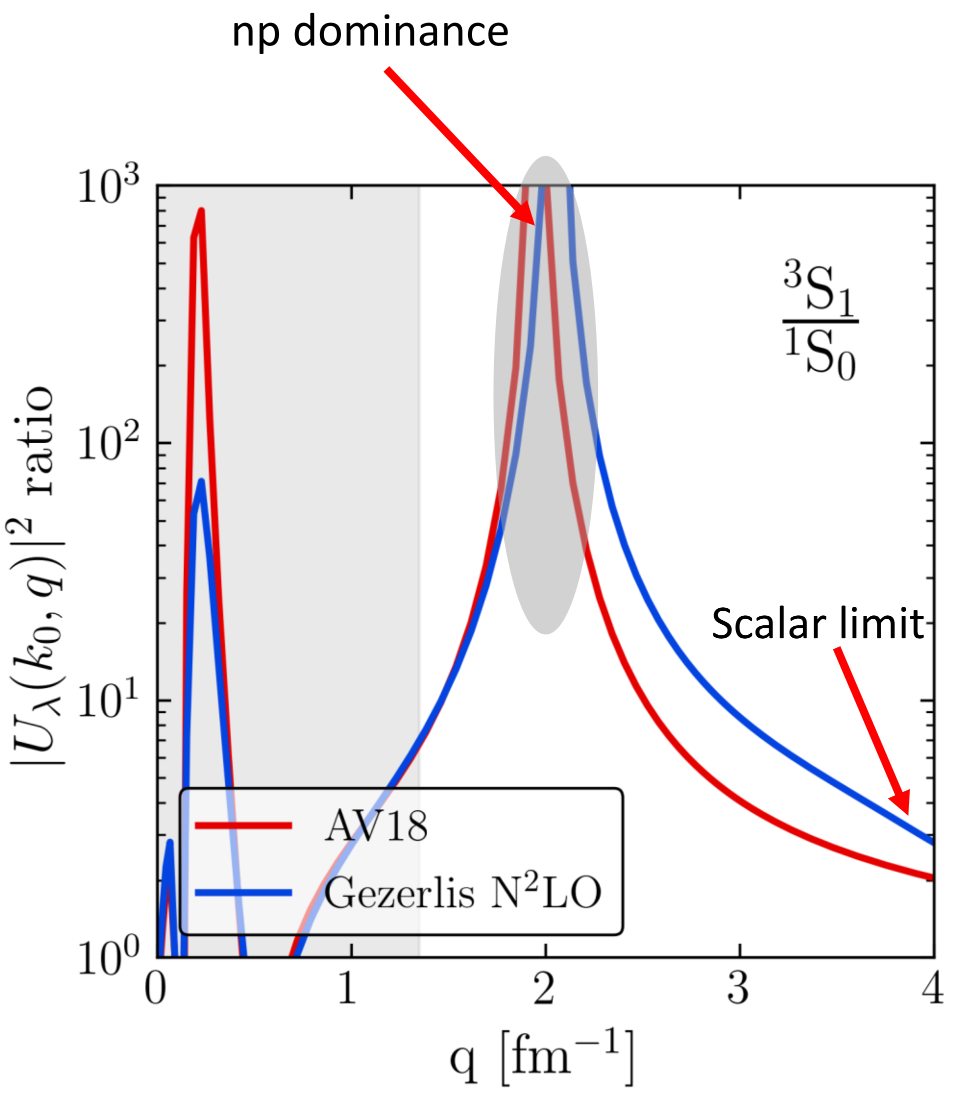

Fig. 11: $^3S_1$ to $^1S_0$ ratio of SRG-evolved momentum projection operators $a^\dagger_q a_q$ where $\lambda = 1.35$ fm^{-1}.

SRC phenomenology

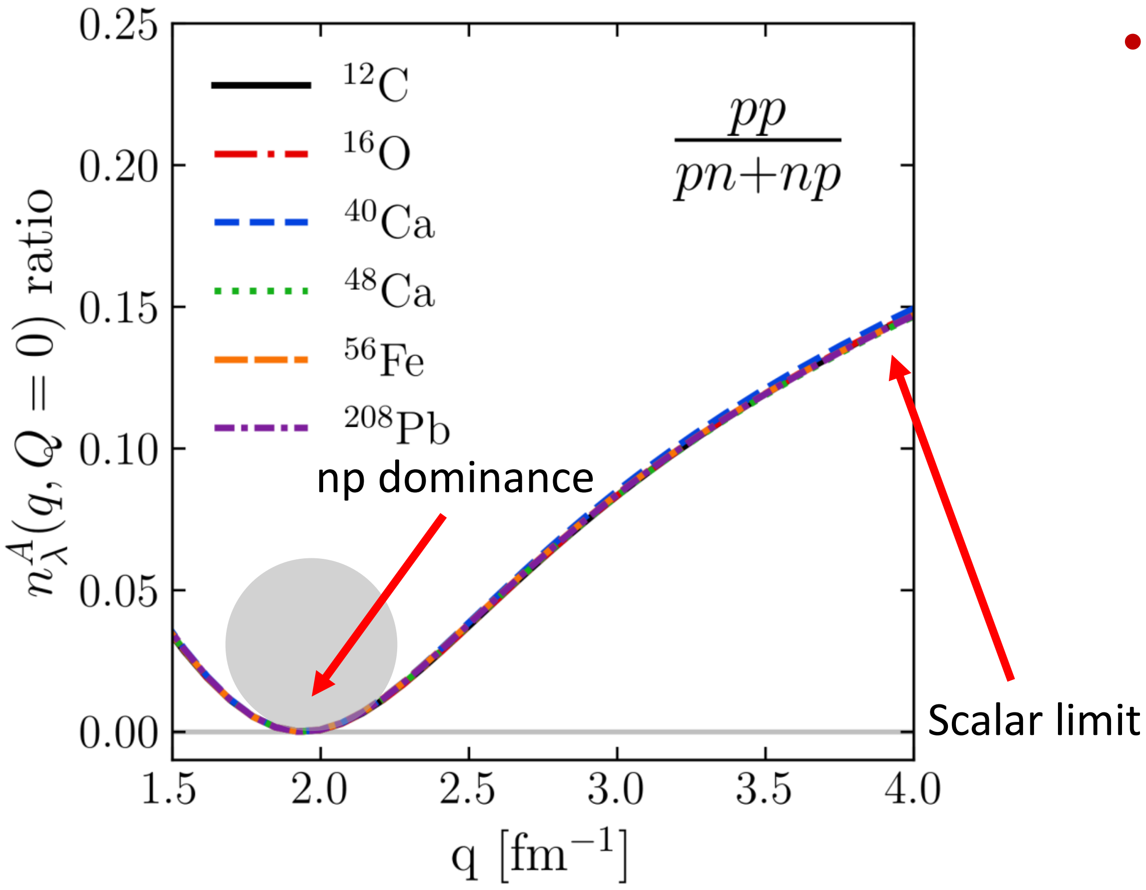

Fig. 12: pp/pn ratio of pair momentum distributions under HF+LDA with AV18 and $\lambda = 1.35$ fm^{-1}.

- Low RG resolution picture reproduces the characteristics of cross section ratios using simple approximations

SRC phenomenology

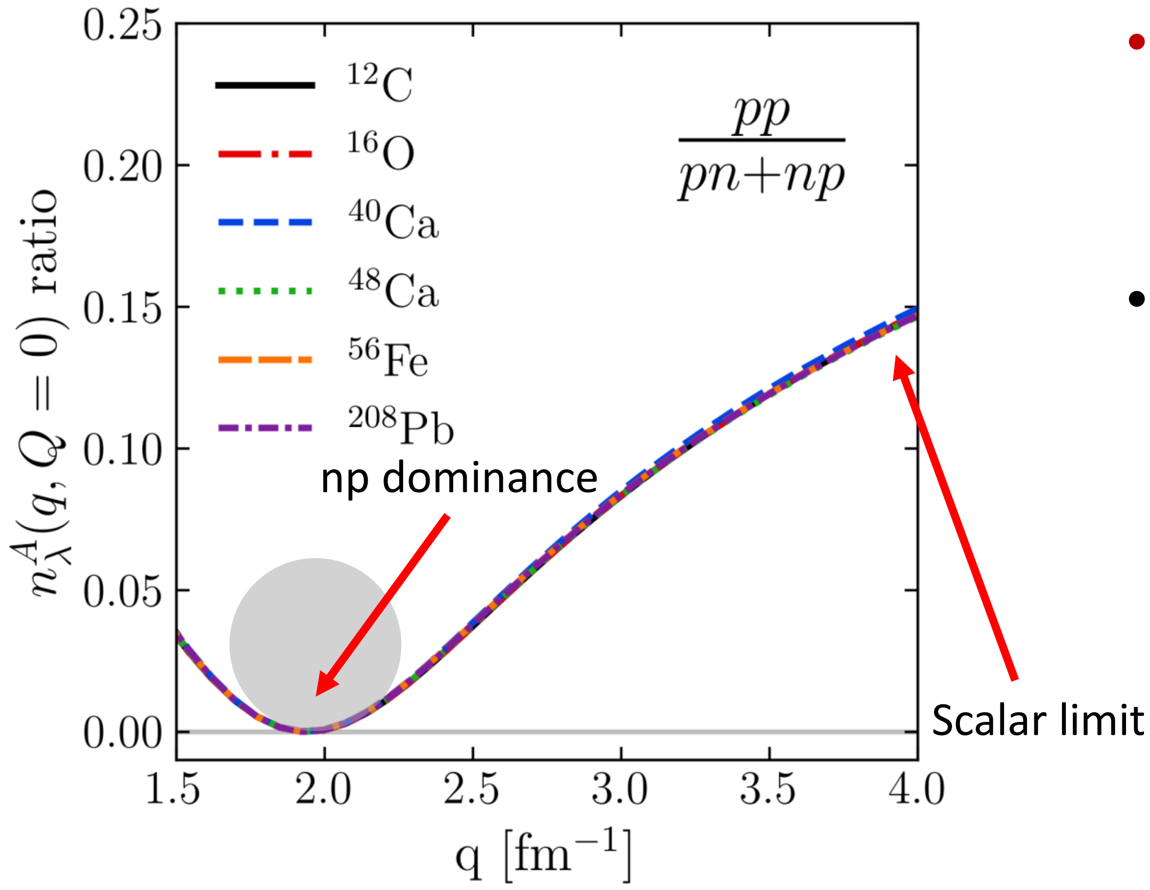

Fig. 12: pp/pn ratio of pair momentum distributions under HF+LDA with AV18 and $\lambda = 1.35$ fm^{-1}.

- Low RG resolution picture reproduces the characteristics of cross section ratios using simple approximations
- Weak nucleus dependence from factorization

$$\text{Ratio} \approx \frac{\left|F_{pp}^{hi}(\boldsymbol{q})\right|^2}{\left|F_{np}^{hi}(\boldsymbol{q})\right|^2} \times \cancel{\frac{\left\langle \Psi_\lambda^A \middle| \sum_{\boldsymbol{k},\boldsymbol{k'}}^{\lambda} a^\dagger_{\frac{\boldsymbol{Q}}{2}+\boldsymbol{k}} a^\dagger_{\frac{\boldsymbol{Q}}{2}-\boldsymbol{k}} a_{\frac{\boldsymbol{Q}}{2}-\boldsymbol{k'}} a_{\frac{\boldsymbol{Q}}{2}+\boldsymbol{k'}} \middle| \Psi_\lambda^A \right\rangle}{\left\langle \Psi_\lambda^A \middle| \sum_{\boldsymbol{k},\boldsymbol{k'}}^{\lambda} a^\dagger_{\frac{\boldsymbol{Q}}{2}+\boldsymbol{k}} a^\dagger_{\frac{\boldsymbol{Q}}{2}-\boldsymbol{k}} a_{\frac{\boldsymbol{Q}}{2}-\boldsymbol{k'}} a_{\frac{\boldsymbol{Q}}{2}+\boldsymbol{k'}} \middle| \Psi_\lambda^A \right\rangle}}$$

SRC phenomenology

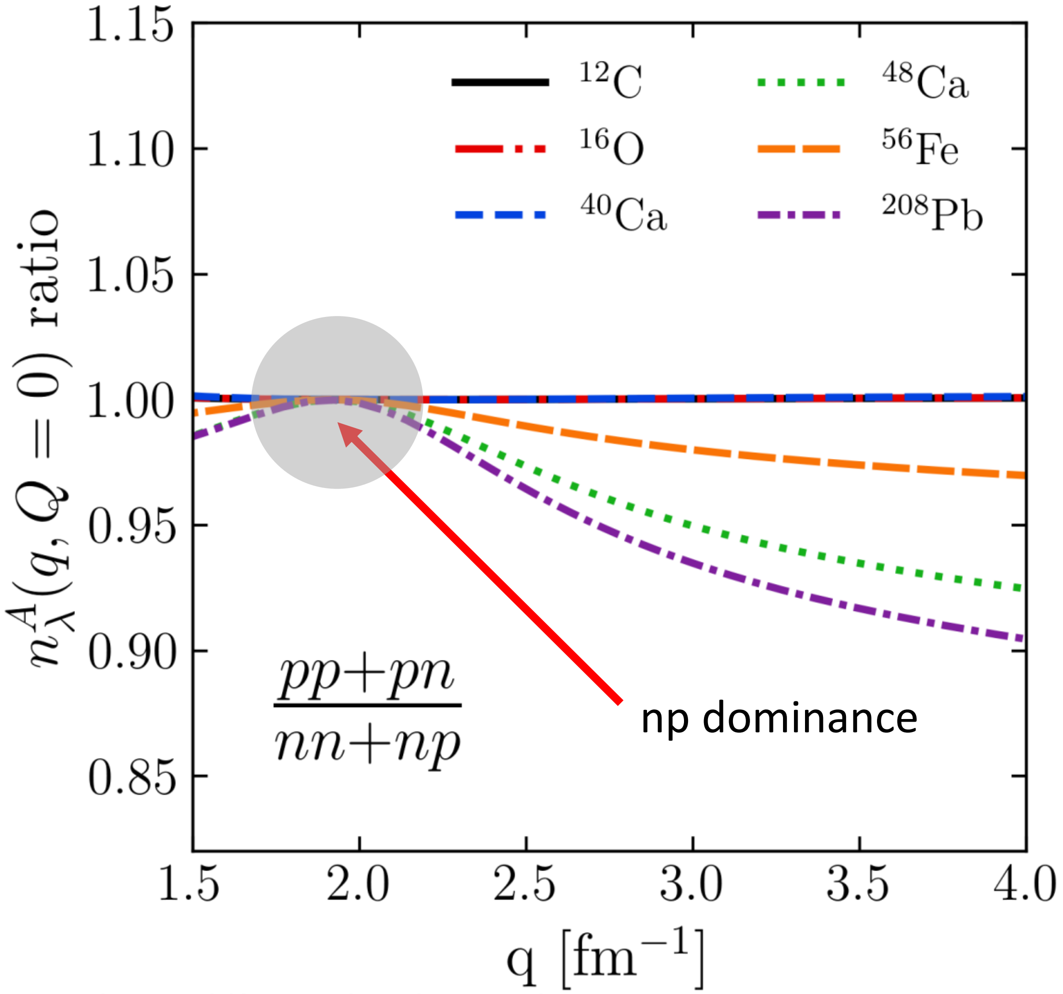

Fig. 13: (pp+pn)/(nn+np) ratio of pair momentum distributions under HF+LDA with AV18 and $\lambda = 1.35$ fm^{-1}.

- Ratio ~1 independent of N/Z in np dominant region
- Ratio < 1 for nuclei where N > Z and outside np dominant region

Exclusive knockout reactions

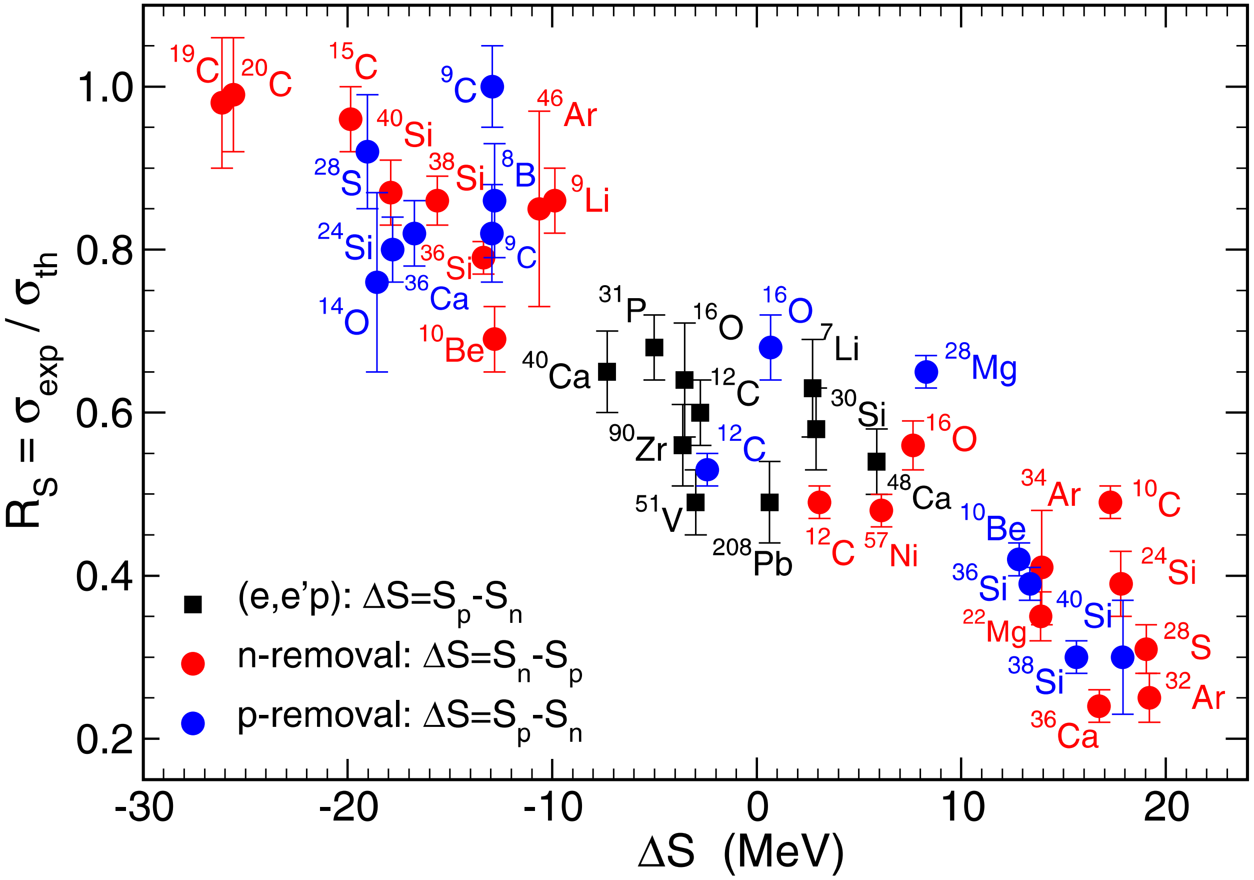

Fig. 14: R as a function of ΔS. Red (blue) points correspond to neutron-removal (proton-removal) cases. Solid black squares correspond to electron-induced proton knockout data. Figure from J. A. Tostevin and A. Gade, Phys. Rev. C **90**, 057602 (2014).

- RG analysis can help understand the cause of $R = \frac{\sigma_{exp}}{\sigma_{theory}} < 1$
- Mismatch of scale between one-body (high RG) operator and shell model structure (low RG) gives $\sigma_{theory} > \sigma_{exp}$

Exclusive knockout reactions

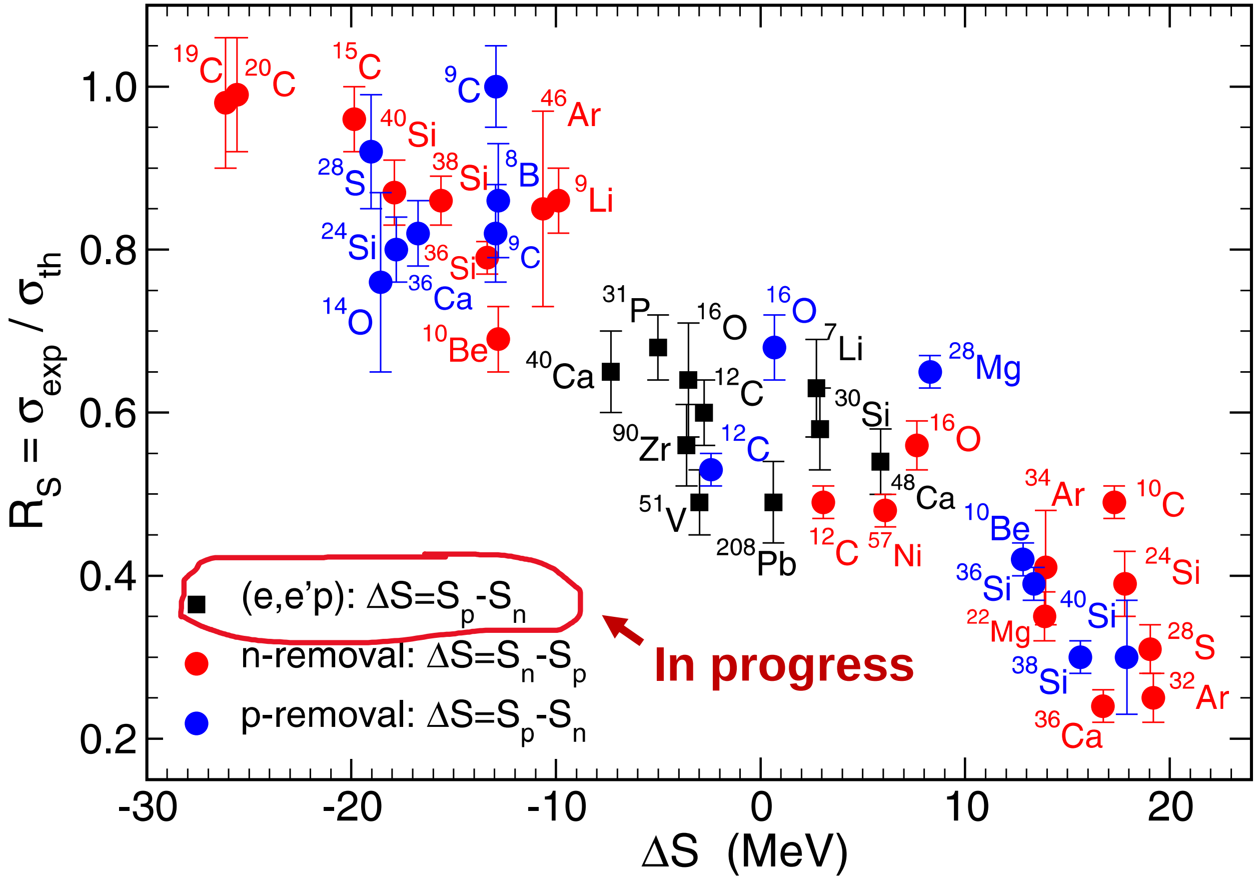

Fig. 14: R as a function of ΔS. Red (blue) points correspond to neutron-removal (proton-removal) cases. Solid black squares correspond to electron-induced proton knockout data. Figure from J. A. Tostevin and A. Gade, Phys. Rev. C **90**, 057602 (2014).

- RG analysis can help understand the cause of $R = \frac{\sigma_{exp}}{\sigma_{theory}} < 1$
- Mismatch of scale between one-body (high RG) operator and shell model structure (low RG) gives $\sigma_{theory} > \sigma_{exp}$
- Currently working on SRG-evolving spectroscopic factors for $(e, e'p)$ reactions
- Note, spectroscopic factors are scale/scheme dependent

Spectroscopic factors

- Spectroscopic factor for single-particle (sp) state α defined in terms of removal amplitude

$$S = \int d\boldsymbol{p} \left| \langle \Psi_\alpha^{A-1} | a_{\boldsymbol{p}} | \Psi_0^A \rangle \right|^{\mathbf{2}}$$

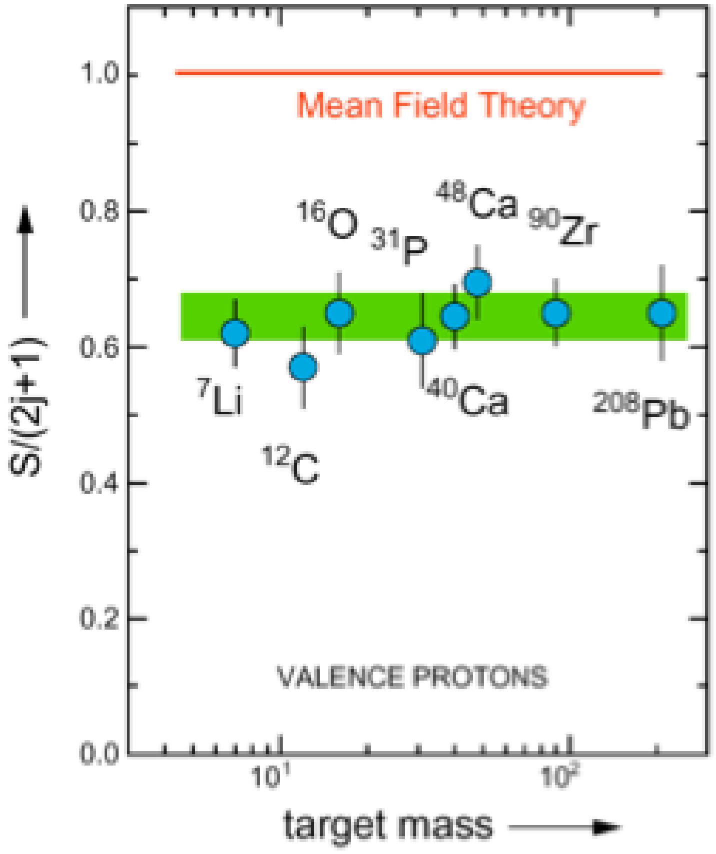

Spectroscopic factors

- Spectroscopic factor for single-particle (sp) state α defined in terms of removal amplitude

$$S = \int d\boldsymbol{p} \left| \langle \Psi_\alpha^{A-1} | a_{\boldsymbol{p}} | \Psi_0^A \rangle \right|^2$$

- sp strength is reduced relative to the independent particle model (IPM) by correlations: Long-range correlations (LRC) and SRC

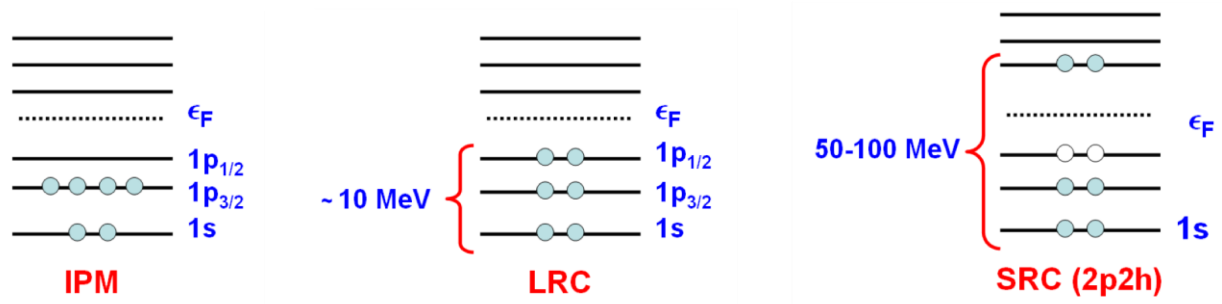

Long-range vs. short-range correlations

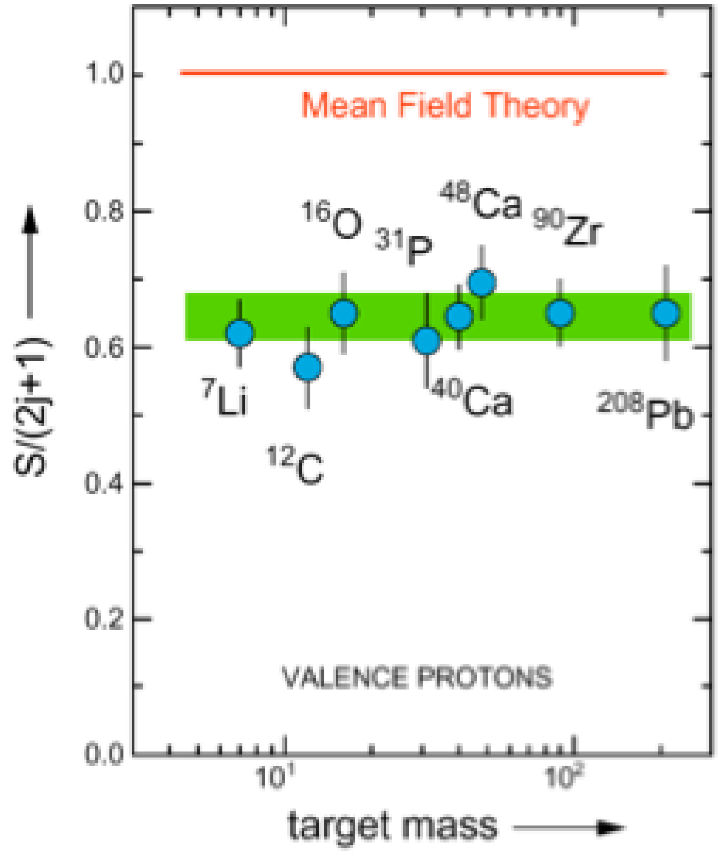

Spectroscopic factors

- Spectroscopic factor for single-particle (sp) state α defined in terms of removal amplitude

$$S = \int d\boldsymbol{p} \left| \langle \Psi_\alpha^{A-1} | a_{\boldsymbol{p}} | \Psi_0^A \rangle \right|^2$$

- sp strength is reduced relative to the independent particle model (IPM) by correlations: Long-range correlations (LRC) and SRC

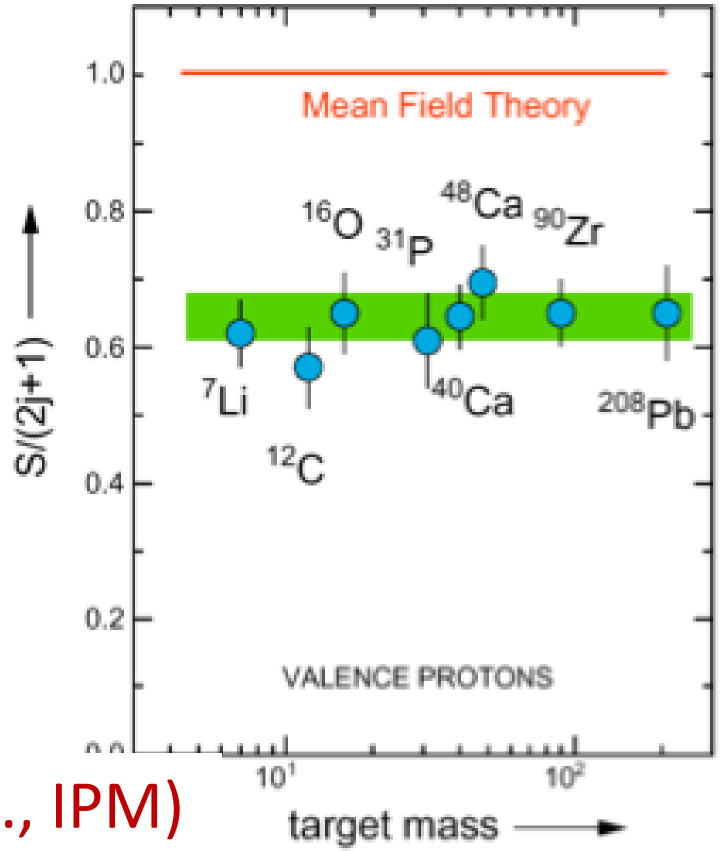

Idea: SRG evolve and analyze using simple approximations (i.e., IPM)

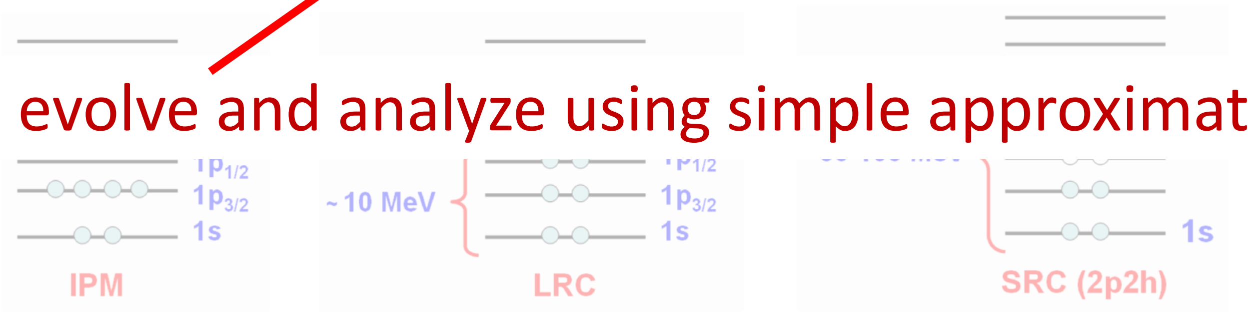

Long-range vs. short-range correlations

Summary and outlook

- At low renormalization group (RG) resolution, simple approximations to SRC physics work and are systematically improvable
- Results suggest that we can analyze high-energy nuclear reactions using low RG resolution structure (e.g., shell model) and consistently evolved operators
  - Matching resolution scale between structure and reactions is crucial!

Summary and outlook

- At low renormalization group (RG) resolution, simple approximations to SRC physics work and are systematically improvable
- Results suggest that we can analyze high-energy nuclear reactions using low RG resolution structure (e.g., shell model) and consistently evolved operators
  - Matching resolution scale between structure and reactions is crucial!
- Ongoing work:
  - Extend to $(e, e'p)$ knockout cross sections and test scale/scheme dependence of extracted properties
  - Investigate impact of various corrections: 3-body terms, final state interactions, etc.
  - Apply to more complicated knock-out reactions (SRG with optical potentials)
  - Implement uncertainty quantification in low RG resolution calculations

Extras

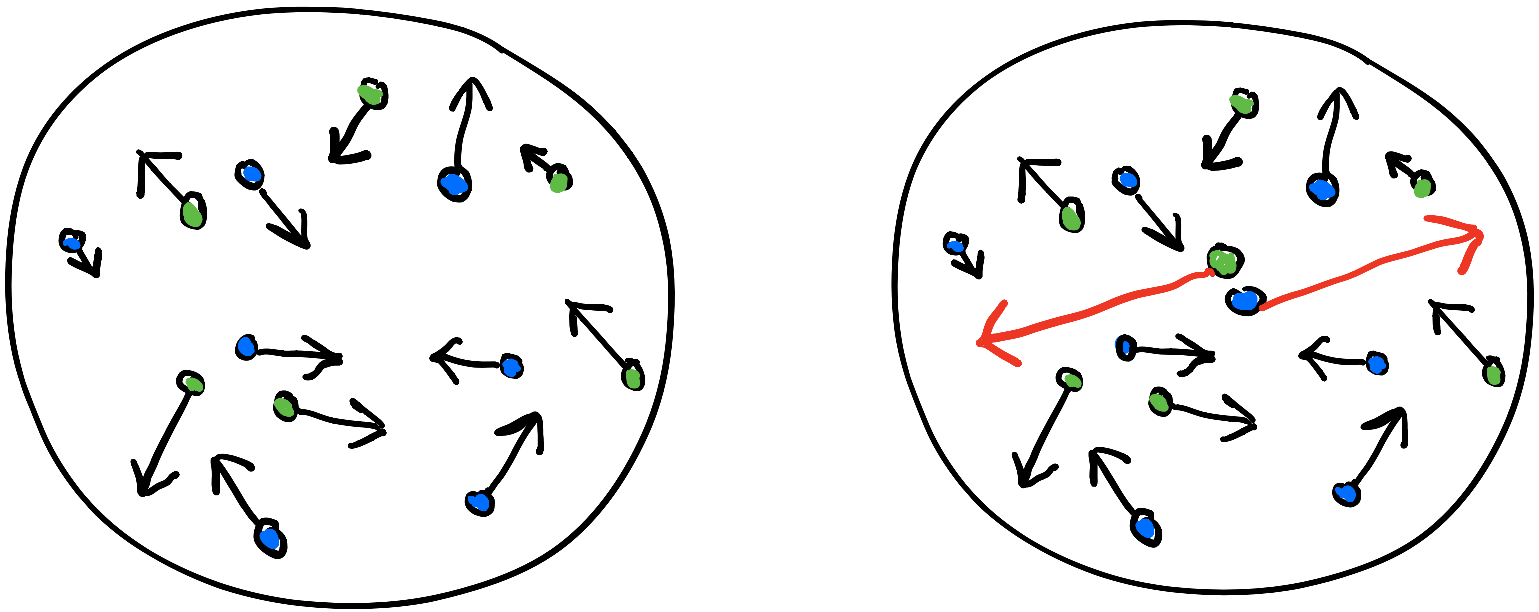

Fig. 10: Cartoon snapshots of a nucleus at (left) low-RG and (right) high-RG resolutions. The back-to-back nucleons at high-RG resolution are an SRC pair with small center-of-mass momentum.